

Recent Advances in the Discovery of CK2 Inhibitors

Mustafa A. Al-Qadhi,* Tawfeek A. A. Yahya, and Hala B. El-Nassan

Cite This: *ACS Omega* 2024, 9, 20702–20719

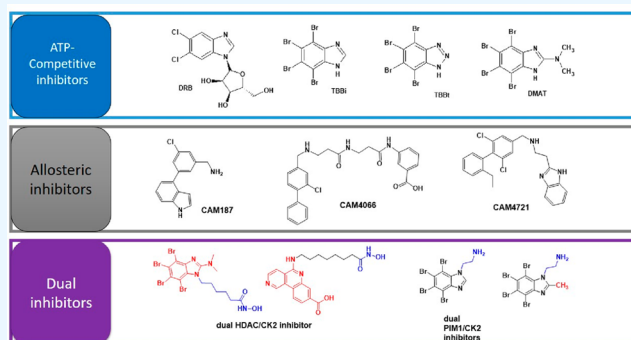
Read Online

ACCESS |

Metrics & More

Article Recommendations

ABSTRACT: CK2 is a vital enzyme that phosphorylates a large number of substrates and thereby controls many processes in the body. Its upregulation was reported in many cancer types. Inhibitors of CK2 might have anticancer activity, and two compounds are currently under clinical trials. However, both compounds are ATP-competitive inhibitors that may have off-target side effects. The development of allosteric and dual inhibitors can overcome this drawback. These inhibitors showed higher selectivity and specificity for the CK2 enzyme compared to the ATP-competitive inhibitors. The present review summarizes the efforts exerted in the last five years in the design of CK2 inhibitors.



INTRODUCTION

The protein kinase CK2 is one of the most important eukaryotic protein kinases (EPKs) that control many processes in the human body. It was first named “casein kinase 2 CK-II”, as it was formerly considered to be the kinase that phosphorylates casein. Later on, it was found that the enzyme does not phosphorylate casein but phosphorylates around 400 other substrates.^{1,2}

CK2 is a constitutively active enzyme formed of two catalytic and two regulatory subunits arranged to form a tetramer. The catalytic subunits are identified as α and α' and are constitutively active, while only one regulatory subunit is identified to date and is known as β . The β subunit aids in maintaining the enzyme stability as well as substrate selection.^{3,4} The structure of CK2 includes many acidic amino acid residues like aspartic (D) and glutamic (E) acids.⁵ The architecture of the CK2 α subunit consists of two main lobes. The small lobe (N-terminal) is rich in β strands and α -helix C, while the large lobe (C-terminal) is formed by the α -helix and is involved in transmitting phosphorus atoms during the phosphorylation process. These two lobes are connected through a short loop, called the “hinge region” which includes the ATP binding site.^{3,6–8}

The unique property for the CK2 kinase family is the ability to use both ATP and GTP as phosphor acceptor/donor because it provides enough space for a hydrogen bonding frame shift at the nucleotide-binding site. The ATP/GTP binding site of CK2 contains at least four important amino acid substitutions: Val66 and Trp176 in the catalytic site and Ile 174 and Met 163 in the hydrophobic region. The bulkiness of these unique CK2 α/α' residues appears to be responsible for

the reduced size and the greater hydrophobicity of the cavity.^{3,6–8}

Another unique characteristic of CK2 is its N-terminal region from Ser7 to Glu36 which plays important role in the CK2 “always active conformation” through phosphorylation of one or more residues (Ser/Thr or Tyr) which are present in the activation loop.⁹ What is more important is the substrate specificity of CK2 which can accept highly acidic protein substrates owing to the presence of 10 basic amino acids in the active site. On the contrary, most other Ser/Thr kinases are basophilic in nature.^{3,6,10}

CK2 enzyme regulates many major pathways such as NF- κ B and STAT3,¹¹ PI3K/Akt,¹² TNF- α ,¹³ and Tyr-kinase receptor.^{13,14} In addition, CK2 can regulate normal and tumor cell proliferation through counteracting caspase effects,¹⁵ potentiating DNA repair¹³ and inhibiting tumor suppressors.¹⁶

Since CK2 phosphorylates a large number of substrates, it can control many functions in the human body and affect many diseases.¹⁷ However, its prominent role in controlling cancer was well investigated. CK2 promotes cell survival, proliferation, and angiogenesis and suppresses apoptosis.^{15,18,19} CK2 has a proven role in antitumor drug resistance.²⁰ Indeed, CK2 has proved to be effective in treating many types of cancer including solid tumors and leukemia.^{21–24} CK2

Received: December 29, 2023

Revised: April 5, 2024

Accepted: April 12, 2024

Published: May 3, 2024



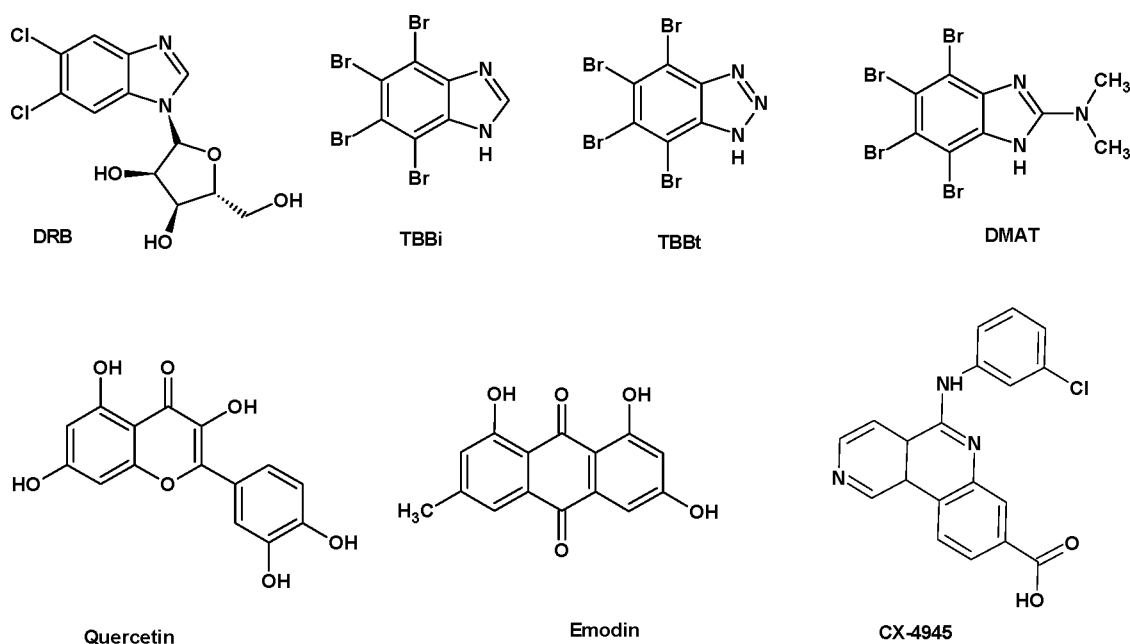


Figure 1. Structures of reported CK2 inhibitors.

inhibitors also prevent metastasis and inhibit angiogenesis and tumor cell invasion.²⁵ In addition, CK2 plays a vital role in the life cycles of bacteria and viruses.^{1,26}

CK2 inhibitors can also be used to treat neurological and psychiatric disorders since CK2 is highly expressed in the brain and mutation of CK2 has been reported in many neurodegenerative disorders.²⁷ These neurodegenerative disorders include Alzheimer disease (AD), Parkinson disease (PD), amyotrophic lateral sclerosis (ALS), and frontotemporal dementia (FTD).²⁸

Two CK2 inhibitors entered clinical trials as anticancer agents named CX-4945 and CIGB-300. CX-4945 (silmisartib, Figure 1) was developed by Cylene Pharmaceutical in 2010.^{18,29} CX-4945 has $K_i = 223$ pM,³⁰ and it showed antiproliferative activity over a wide panel of cancer cell lines.³¹ CX-4945 was granted as an orphan drug by the U.S. Food and Drug Administration.³² The drug is orally available with acceptable safety and pharmacokinetic properties.^{33,34} Its ability to cross the blood–brain barrier can make it suitable to treat brain tumors and other brain related diseases.³⁵ This compound entered clinical trials in phase I/II on patients with cholangiocarcinoma (ClinicalTrials.gov identifier: NCT02128282), metastatic basal cell carcinoma (BCC; ClinicalTrials.gov identifier: NCT03897036), recurrent SHH (sonic hedgehog) medulloblastoma (ClinicalTrials.gov identifier: NCT03904862), multiple myeloma (ClinicalTrials.gov identifier: NCT01199718), and breast cancer (ClinicalTrials.gov identifier: NCT00891280). During the corona virus epidemic (SARS-CoV-2), silmisartib emerged as a possible treatment for severe acute respiratory syndrome (ClinicalTrials.gov identifier: NCT04668209).³⁶

CX-4945 inhibited other kinases with IC_{50} values less than 100 nM, such as DYRK1A, DYRK1B, DYRK3, CDK1, PIM1, CLK1–CLK3, FLT3, DAPK3, TBK1, and HIPK3. This resulted in unwanted off-target effects in the clinical trials.^{30,37,38} It is postulated also that the anticancer activity of CX-4945 is attributed to the off-target inhibition of these enzymes.²⁹

The peptide CIGB-300 was developed by Perea and collaborators for treatment of cervical malignancies. This compound selectively inhibits certain CK2 substrates and cannot be considered as a global CK2 inhibitor. The results of the clinical trials indicated that the compound had decreased squamous intraepithelial lesion in 90% of the patients with good tolerability and minor side effects, while in a phase I trial on women with locally advanced cervical cancer the compound induced histamine release.^{25,39–41} Another peptide-based CK2 inhibitor that was used for COVID-19 treatment was the peptide derivative CIGB325, an anti-CK2 peptide.⁴²

CK2 INHIBITORS

The present review summarizes the efforts done in the last five years (2019–2023) in the drug design and discovery of CK2 inhibitors. The inhibitors can be classified as ATP-competitive, allosteric, and dual inhibitors.

ATP-Competitive Inhibitors. The ATP pocket of CK2 is small and narrow compared to other kinases due to the presence of large amino acid residues around the pocket. Therefore, CK2 can effectively bind small compounds in the ATP binding site which are loosely fit in the ATP of other kinases. This results in higher specificity and selectivity of the CK2 ATP-competitive inhibitors over other kinases.⁴³

Examples of this class include the polyhalogenated benzimidazole derivatives: DRB,⁴⁴ TBB,⁴⁵ TBI (also called K17), and DMAT (also called K25)⁴⁶ (Figure 1). Some natural compounds showed CK2 inhibition such as flavonoids like apigenin and quercetin,⁴⁷ anthraquinone like emodin and quinalizarin,⁴⁸ and curcumin.⁴⁹ CX-4945 is the only ATP-competitive inhibitor in clinical trials^{33,34} (Figure 1).

The ATP binding pocket of the CK2 enzyme includes three main regions; the hinge region that connects the N-terminal and C-terminal lobes of the enzyme and is formed of 114–120 amino acids, the phosphate binding region that contains the Lys68 backbone, and the hydrophobic area. The latter is centered between the hinge region and the phosphate binding

region and includes Val53, Val66, Ile95, Phe113, Met163, and Ile174 residues.⁵⁰

The crystal structure of human CK2 in complex with CX-4945 was determined for the first time in 2011 by Battistutta et al. (PDB ID 3PE1; Figure 2).^{30,51} The results indicated that

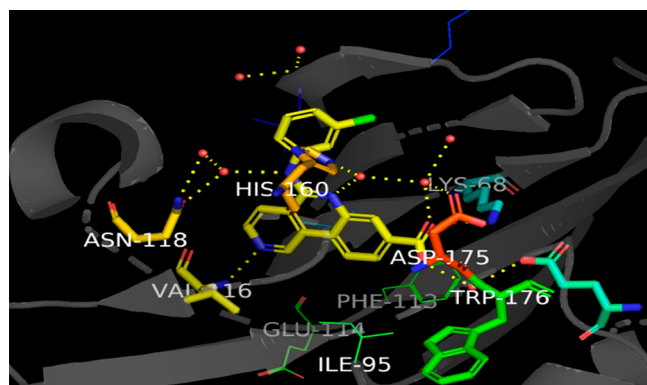


Figure 2. X-ray cocrystal structure of CX-4945 with CK2 (PDB ID 3PE1; 1.60 Å). The figure was generated using PyMOL 2.4.0 with the CK2 α protein shown as a cartoon and CX-4945 shown as sticks colored by the atom type: C, yellow; O, red; and N, blue. The H-bonds are illustrated in yellow dashed lines. The bound water molecules are shown as red spheres.

the compound fit in the CK2 active site and interacted with the ATP cavity of both CK2 α and CK2 α' . The pyridine nitrogen atom of CX-4945 made an H-bond with a Val116 residue of the CK2 hinge region. Additionally, the carboxylate group interacted via a water molecule with Lys68, Glu81 from gatekeeper β 3 and β 4 of α C from the N lobe, Asp175, Ile174, and Trp176 from DFG, and the activation segment of the C lobe. Moreover, two H-bonds were observed between the nitrogen of the benzo-naphthyridine scaffold and the His160 residue and between the amino group of chlorophenyl and Asn118 through a water molecule. On the basis of these crystal structures, it was recognized that the fundamental features of an ATP-competitive CK2 inhibitor are appropriate hydrophobicity, excellent shape complementarity with the unique and small active site for the presence of bulky residues such as gatekeeper residue Phe113, and the unique Val66 and Ile174.

In 2023, Davis-Gilbert et al. optimized CX-4945 (silmitasertib) through replacement of a pyridine ring and the 3-chlorophenyl ring with pyrimidine and a benzyl ring, respectively, to afford a potent and selective naphthyridine-based chemical probe for CK2, **1** (IC_{50} = 3 nM) (Figure 3).⁵²



Figure 3. Structure modification of CX-4945 to afford compound **1**.

SAR study indicated that both pyridine and pyrimidine rings can bind to the hinge region, resulting in potent CK2 inhibitors. In addition, pyrimidine derivatives showed better cell permeability and selectivity than pyridine analogues. The replacement of a phenylamino with a benzylamino group enhanced the selectivity as well. On the other hand, the removal of carboxylic acid at C-7 resulted in an inactive

compound. The binding mode of compound **1** within the active site of CK2 α (PDB ID 8BGC) revealed that a hydrogen bond was formed between pyrimidine nitrogen and the backbone NH between His115 and Val116. Additional hydrogen bonds were formed between the carboxylic acid and Lys68, a water mediated with Glu81 on the α C helix, and a backbone NH adjacent to Asp175 from the DWG motif. The π -stacking interaction between the phenyl ring and His160 was observed (Figure 4).⁵²

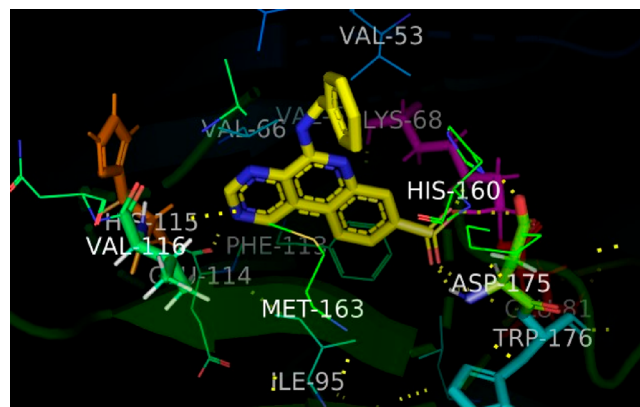


Figure 4. X-ray cocrystal structure of compound **1** with CK2 (PDB ID 8BGC; 2.80 Å). The figure was generated using PyMOL 2.4.0 with the CK2 α protein shown as a cartoon and compound **1** shown as sticks colored by the atom type: C, yellow; O, red; and N, blue. The H-bonds are illustrated in yellow dashed lines.

The pyrazolopyrimidine inhibitor **3** (SGC-CK2-1, Figure 5) was identified by Wells et al. in 2020 as a highly potent CK2 inhibitor.^{53,54} The amide group was responsible for the effective binding to the enzyme. Compound **3** was identified through structure modification of the lead compound **2**. This was achieved by replacing the cyclopropanecarboxamide group with acetamide (compound **4**) or propionamide (compound **3**). On the other hand, it was observed that N-methylation as in compound **5** reduced the inhibitory activity significantly. Compound **3** represented a highly potent CK2 inhibitor with specific selectivity for both human CK2 isoforms (IC_{50} = 36 and 16 nM on CK2 α and CK2 α' , respectively). However, this compound was devoid of antitumor activity against a panel of 140 cancer cell lines. Only U937, the human myeloid leukemia cell line, was sensitive to compound **3**. Nevertheless, this derivative could be good candidate for the treatment of neurodegenerative diseases and viral infections that require selective CK2 inhibitor.^{53,54}

In another study, structure optimization of SGC-CK2-1 (compound **3**) was achieved by replacing the methyl group with a morpholine ring as a solubilizing moiety and changing the propionamide group with an acetamide group to decrease the lipophilicity. This optimization was aimed to improve solubility and metabolic stability. These efforts led to the identification of compound **6** (Figure 5), which exhibited potent antiviral activity with moderate rates of clearance in human primary hepatocytes.⁵⁵

The X-ray crystal structure compound **3** in the ATP binding site of CK2 [PDB ID 6Z83, Figure 6] indicated that the pyrazolopyrimidine core and 7-cyclopropylamine bind to Val116 in the hinge region. The propionamide group formed two H-bonds with the amino acid residues Lys68 and Asp175.

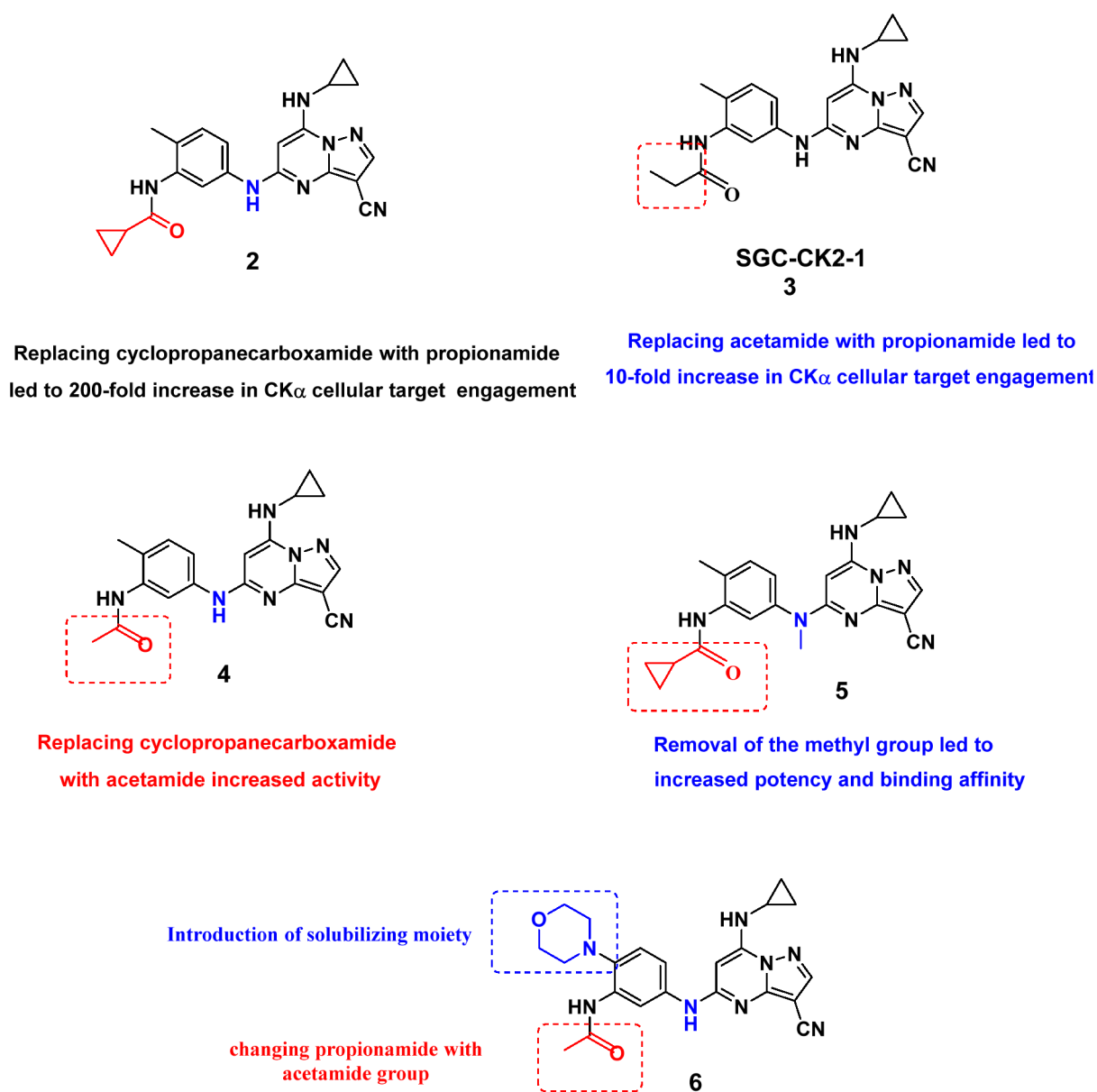


Figure 5. Design of compounds 2–6.

Other water mediated H-bonds were formed between Asn118, Ile95, and the phenylamino NH group.^{53,54} Insertion of the *N*-methyl group at position 5 resulted in a steric clash with the ATP site in the region of Met168, and that distorted the orientation of the pyrazolopyrimidine core and prevented effective binding to the hinge region.^{53,54}

On the basis of this crystal structure, it was recognized that the fundamental features of an ATP-competitive CK2 inhibitor were appropriate hydrophobicity, excellent shape complementarity with the unique and small active site, and the ability to establish polar interactions with both of the two main anchoring sites: the Val116 backbone at the beginning of the hinge region and the positive electrostatic area near the conserved water W1 and Lys68.^{53,54}

Krämer et al.⁵⁶ also explored the pyrazolo[1,5-*a*]pyrimidine hinge-binding moiety for the development of selective CK2 inhibitors. Optimization of this scaffold produced the acyclic **7** and the macrocycle **8** derivatives (Figure 7), which shared a carboxylic acid group at the pendant aromatic ring as well as a

Boc group located at the amine attached to the 5 position of the pyrazolo[1,5-*a*]pyrimidine. These variations were essential for potent and selective binding to CK2 α . The most potent compound **7** had IC₅₀ = 8 nM on CK2 α , comparable to CX-4945, and IC₅₀ = 38 nM on CK2 α' . Moreover, both compounds were assessed for their selectivity against a larger kinase panel at a concentration of 1 μ M. Compound **7** exhibited POCs (percent of control) of less than 10% against kinases CSNK2A2, CSNK2A1, and DAPK2, whereas compound **8** gave POCs of less than 2% against kinases INSR, PIM3, EGFR, CSNK2A2, and PIK3CA and gave POCs of 5–10% against kinases BMPR2, BUB1, MAP3K12, and MAPK15. However, compound **7** did not exhibit any significant effect on 60 cancer cell lines, probably due to its poor cell penetration.⁵⁶

The presence of more polar functional groups in compounds **7** and **8** afforded better interactions with CK2 residues. The presence of a carboxylic group was essential for the inhibitory activity. The binding modes of the acyclic and macrocyclic compounds were identical (Figure 8). The carboxylate group

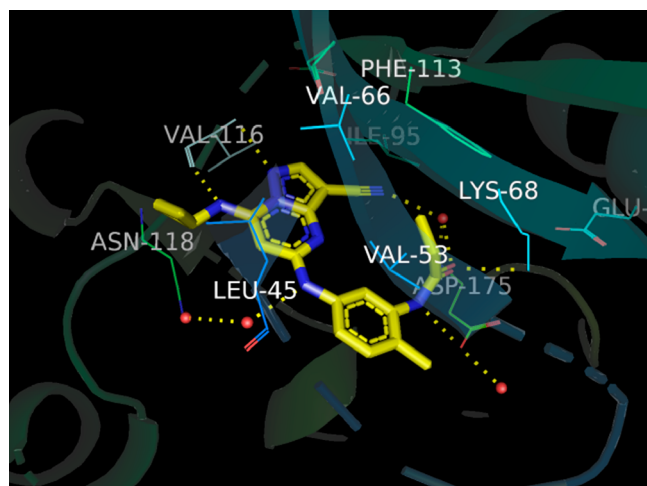


Figure 6. X-ray cocrystal structure of compound 3 with CK2 α (PDB ID 6Z83; 2.17 Å). The figure was generated using PyMOL 2.4.0 with the CK2 α protein shown as a cartoon and compound 3 shown as sticks colored by the atom type: C, yellow; O, red; and N, blue. The H-bonds are illustrated in yellow dashed lines. The bound water molecules are shown as red spheres.

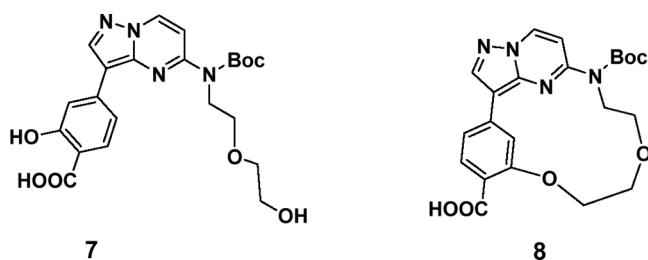


Figure 7. Structures of compounds 7 and 8.

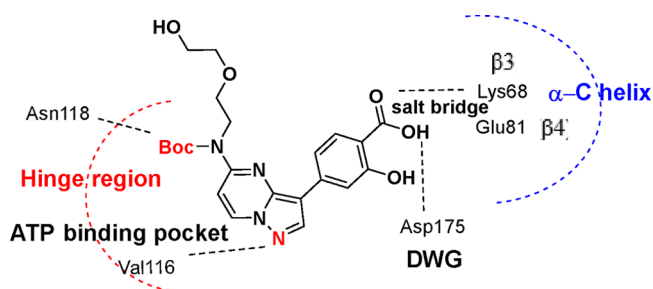


Figure 8. Key interactions between compound 7 and CK2 residue inside active site.

formed salt bridges to Lys68 and a water mediated H-bond with Glu81. Another H-bond was formed with the nitrogen of Asp175, which is a part of the degenerated DFG (DWG) motif in CK2. The carbonyl group of the Boc group formed an additional H-bond to the Asn118 at the hinge region which accounted for the higher affinity observed with compounds containing Boc groups. The orientations of the pyrazolo[1,5-*a*]pyrimidine ring system and the pendant 3-phenyl ring were similar in the open and cyclized compounds. This explained the comparable inhibitory activity and selectivity profiles noticed with compounds 7 and 8.⁵⁶

In 2022, Urakov et al. described the design and structure–activity relationship of 6-(tetrazol-5-yl)-7-aminoazolo[1,5-*a*]pyrimidines 9 and 10 as CK2 inhibitors (Figure 9). The SAR

study demonstrated that the 3-phenyl analogue 10 exhibited potent inhibition against CK2 with an IC₅₀ value of 45 nM.⁵⁷

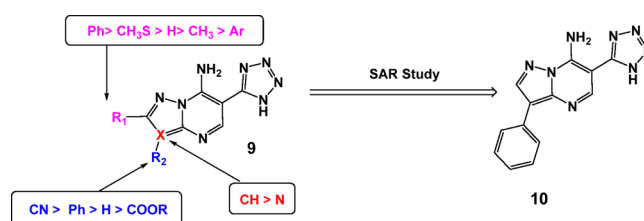


Figure 9. Design of compounds 9 and 10.

Chojnacki et al. designed and synthesized 1*H*-triazolo[4,5-*b*]pyridines and 1*H*-imidazo[4,5-*b*]pyridines as analogues of two potent CK2 inhibitors, namely 4,5,6,7-tetrabromo-1*H*-benzimidazole (TBBi) with IC₅₀ = 1.3 μM and 4,5,6,7-tetrabromo-1*H*-benzotriazole (TBBt) with IC₅₀ = 0.3 μM.⁵⁸ Previously published studies on the role of halogen atoms, especially the bromine atom in TBBt, on the inhibitory activity revealed that the bromine atoms at the C5 and C6 positions were essential for CK2 binding, while modifications at positions C4 and C7 of TBBt can lead to more effective inhibitors of CK2.⁵⁹ Similarly, the removal of one bromine atom from the structure of TBBi reduced the affinity to the CK2 enzyme.⁶⁰

Chojnacki et al. modified the structure by adding the pyridine nitrogen atom instead of the bromine atom at position 4 in both compounds. Then, the bromine atom at position 7 was removed and that at position 5 was replaced with a chlorine atom to examine the effect of the number and position of halogens on the CK2 inhibitory activity and selectivity.⁵⁸ These modification afforded the 1*H*-triazolo[4,5-*b*]pyridine derivatives (11–13, Figure 10) which were more active than the 1*H*-imidazo[4,5-*b*]pyridine derivatives (14–16, Figure 10). Interestingly, the 1*H*-triazolo[4,5-*b*]pyridines containing two halogen atoms, either two bromine (compound 12) or chlorine and bromine (compound 13), were the most potent CK2 α inhibitors with IC₅₀ = 2.56 and 3.26 μM, respectively. Compound 11 with three bromine atoms showed CK2 α inhibition with IC₅₀ = 3.82 μM.⁵⁸ In addition, some differences could be observed in the inhibition of PIM1 kinase. Compounds bearing two halogen atoms (12 and 13) did not inhibit the activity of PIM1. On the contrary, compounds having three bromine atoms (11 and 14) showed moderate inhibitory activity against PIM1. This might be explained in the view of the sizes of the molecules and active site dimensions of the two different kinases. However, all the compounds did not exhibit any cytotoxic effect upon testing on MCF-7 and CCRF-CEM cell lines.⁵⁸

Figure 11 displays the main interactions of TBBt and TBBi inside the CK2 active site. The bromine atoms at positions 5 and 6 of both compounds interact with Glu114 and Val116. Meanwhile, the nitrogen atom of imidazole or triazole formed an H-bond to the backbone of Lys68 or a water mediated H-bond with Glu81.⁵⁸

Another study based on heterocyclic halogenated compounds was conducted by Winiewska-Szajewska et al., who studied six halogenated ligands derived from commercial 4,5-dihalobenzene-1,2-diamines. The tested compounds included the benzothiadiazole, benzimidazole, and quinoxaline derivatives.⁶¹ Docking study and low-volume differential scanning fluorimetry (nanoDSF) methods were initially done to select

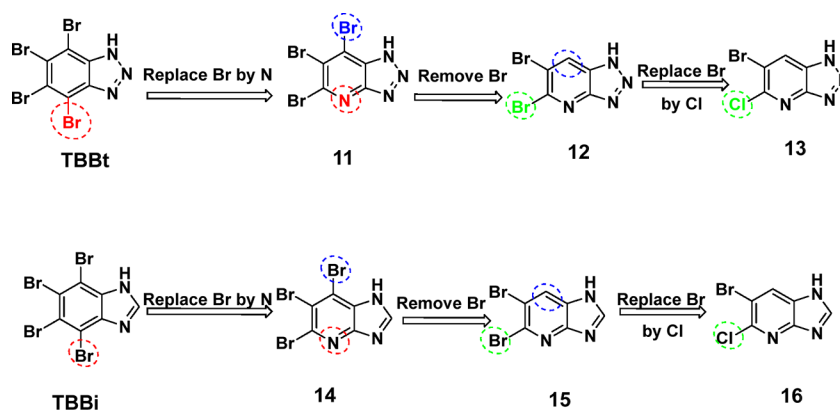


Figure 10. Design of compounds 11–16.

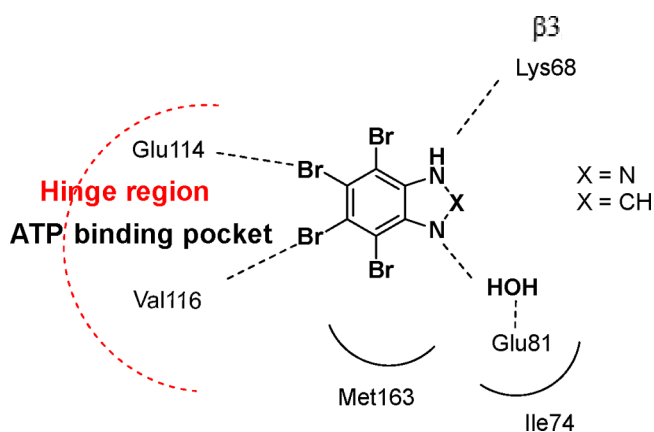


Figure 11. Key interactions of tetrabromo-1*H*-benzimidazole (TBBi) and tetrabromo-1*H*-benzotriazole (TBBt) within CK2 pocket.

the most active scaffold that can fit well in the ATP binding site of CK2. The major factors that control the scaffold binding were the steric hindrance, the electrostatic effects, and the hydrophobic effects. The docking studies suggested that the iodinated ligands preferably adopted the orientation in which both halogen atoms were solvent-protected and were close to the hinge region. The heterocyclic ring pointed toward the polar region of the ATP binding site formed by side chains of Lys68, Glu81, and Asp175.⁶¹ Among the tested compounds, the iodinated derivatives 5,6-diiodo-2-trifluoromethyl-1*H*-benzimidazole (compound 17) and 6,7-diiodoquinoxaline-2,3-diol (compound 18, Figure 12) exhibited the highest

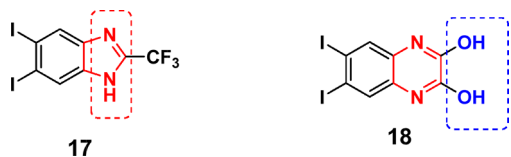


Figure 12. Structures of compounds 17 and 18.

CK2 α inhibitory activity with $IC_{50} = 7$ and $2 \mu M$, respectively.⁶¹ Compound 17 showed higher anticancer activity on four cancer cell lines, epidermoid carcinoma A-431, colorectal carcinoma HCT116, HCT116p53^{-/-}, and normal fibroblasts BJ, than compound 18. The anticancer activity was correlated to the compound hydrophobicity rather than to its inhibitory activity.⁶¹

Dalle Vedove et al.⁵⁰ reported the synthesis and evaluation of CK2 inhibitors containing the 2-cyano-2-propenamide scaffold. The compounds were designed based on the structure of 6-methylene-5-imino-1,3,4-thiadiazolopyrimidin-7-one (SRPIN803, compound 19, Figure 13), which was previously reported as a dual inhibitor of SRPK1 and CK2 enzymes with IC_{50} values of 2.4 and 203 nM, respectively.⁶² However, careful examination of the X-ray crystal structure indicated that its correct structure was the open form (SRPIN803-rev, compound 20). Further structure optimization of the latter compound was done by varying the substituents on the thiadiazole ring to afford compound 21 with an IC_{50} of 280 nM against CK2 α . Compound 21 was quite selective to CK2 and CK2 α' over 320 kinases. Compound 21 exhibited an anticancer effect on the human leukemia T-cell line named Jurkat cells which could be related to the compound's good cell permeability.⁵⁰ The X-ray crystallographic data of compound 20 revealed the CK2 open hinge conformation which is rare in kinases and showed that the side chain bound to the CK2 α hinge region.⁵⁰

The binding mode of compound 21 is displayed in Figure 14. The compound was bound to the hinge region through water mediated H-bonds between the propenamide carbonyl oxygen and Glu114 and Val116. Meanwhile, the guaiacol moiety formed H-bonds with the Lys68 side chain, with Asp175, and with a conserved water molecule that was held in position by the Trp176 main chain amide nitrogen and the Glu81 side chain. The central 2-cyano-2-propenamide moiety formed van der Waals and hydrophobic interactions with the apolar residues lining the cavity. Finally, the thiadiazole ring was sandwiched between the side chains of Leu45 and Asn118, while the bromine group was held in between the hinge region and the N-terminal lobe.⁵⁰

In 2023, new purine derivatives were identified as CK2 α inhibitors based on the solvent dipole ordering based method for virtual screening.⁶³ Docking and SAR studies of the prepared compounds indicated that three groups on the purine scaffold were essential for the inhibitory activity. These groups were the 4-carboxyphenyl group at position 2, the carboxamide group at position 6, and the electron-rich phenyl group at position 9. Compound 22 (Figure 15) was initially identified as a lead compound with $IC_{50} = 12 \mu M$. The most potent compound in this work was derivative 23, which exhibited CK2 α inhibition with $IC_{50} = 4.3 \mu M$.⁶³ The binding mode of compound 23 (Figure 16) indicated that the carboxamide at the 6 position of the purine scaffold was expected to form H-

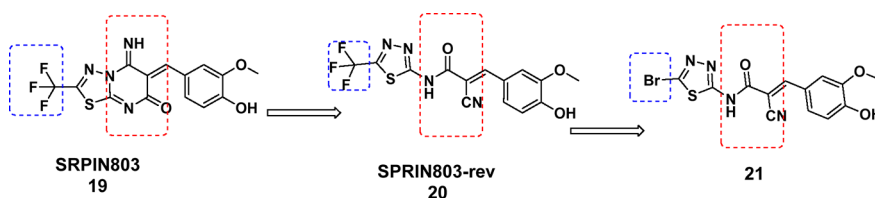


Figure 13. Design of compound 21.

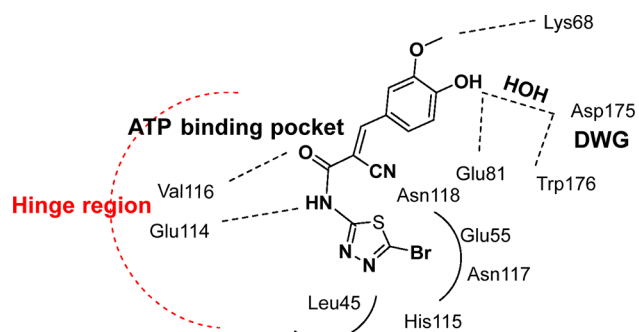


Figure 14. Main interaction between compound 21 and CK2 pocket.

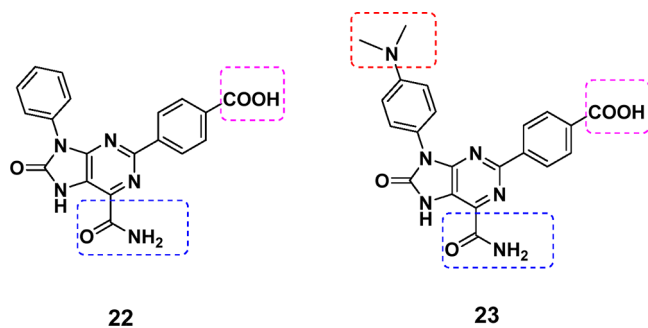


Figure 15. Structures of compounds 22 and 23.

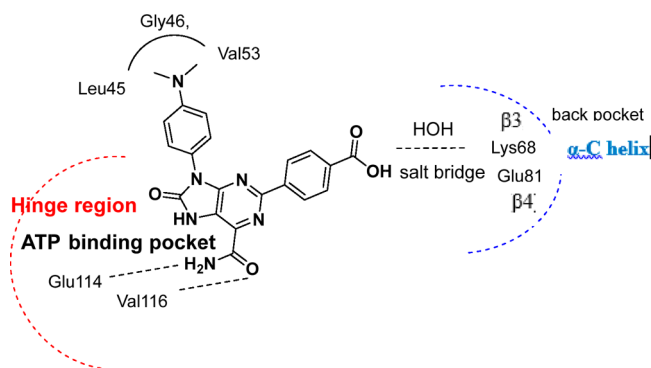


Figure 16. Main interaction between compound 23 and CK2 pocket.

bonds with Glu114 and Val116 in the hinge region, while the carboxyphenyl group at the 2 position of compound 23 was located near Lys68 and Glu81. Finally, the phenyl ring at the 9 position formed a CH- π interaction with hydrophobic residues, such as Leu45, Gly46, and Val53, which accounted for the higher inhibitory activity of this compound.⁶³

The natural anthraquinone derivative endocrocin (Figure 17), which is structurally similar to emodin, was investigated as a CK2 inhibitor. Endocrocin displayed moderate CK2 inhibitory activity with an IC_{50} value of 6 μ M, whereas that of emodin was 2 μ M. This might be attributed to the presence of the carboxylic group in endocrocin that prevented efficient binding to Lys68. Structure modification of endocrocin was performed by López-Rojas and co-workers⁶⁴ leading to the development of 1-amino-6-methylanthracene-9,10-dione (compound 24, Figure 17) as a potent CK2 inhibitor with an IC_{50} value of 1.45 μ M. However, the cellular effect of compound 24 on the MCF7 cell line was weak. SAR study of this series of compounds indicated that the hydroxy groups on ring A were essential for the inhibitory activity.⁶⁴

In 2019, Bestgen et al.⁶⁵ identified the mechanism of action of aryl 2-aminothiazoles (Figure 18) as a novel class of CK2

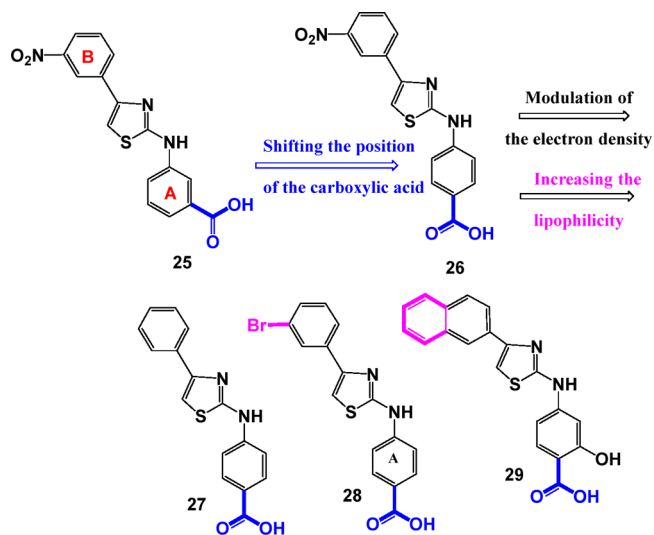


Figure 18. Design of compounds 26–29.

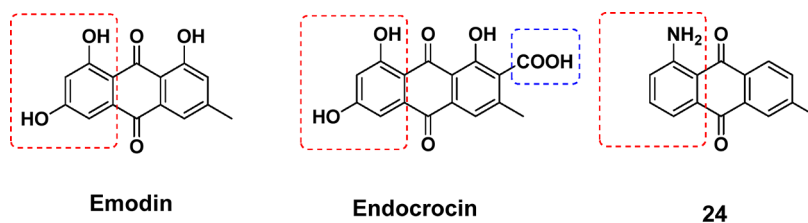


Figure 17. Structures of emodin, endocrocin, and compound 24.

inhibitors. The authors reported that these compounds bound in an allosteric pocket outside the ATP binding site. The combination of alanine scan mutational analysis, the native mass spectrometry based detection and enzyme kinetics (STD-NMR), and molecular docking studies confirmed the finding of a new binding site (allosteric site) of CK2 according to the authors' suggestions. Preliminary SAR study was done to optimize the 2-aminothiazole scaffold **25** ($IC_{50} = 28 \mu M$). The SAR studies demonstrated that the carboxylic acid group (ring A) was very important for ionic bonding with the basic amino acid residue in CK2 and had to be located in the *para* position for optimum activity as with compound **26** ($K_i = 1.6 \mu M$, $IC_{50} = 7 \mu M$). Modulation of both the electron density and lipophilicity of substituents on aromatic ring B was studied. The electron density did not affect the activity (compound **27** had $IC_{50} = 9 \mu M$), whereas the lipophilicity significantly enhanced the binding affinity ($K_i = 0.7 \mu M$) and the inhibitory activity (compound **28** had $IC_{50} = 3.4 \mu M$). It was suggested that this lipophilic moiety formed a hydrophobic interaction with the lipophilic pocket of CK2.⁶⁵ The authors used a structure optimization strategy for compound **25** to generate the allosteric CK2 inhibitor **29** (Figure 18). Compound **29** exhibited good potency against CK2 α ($IC_{50} = 0.6 \mu M$, $K_d = 0.6 \mu M$) and induced apoptosis and cell death in 786-O renal cell carcinoma cells ($EC_{50} = 5 \mu M$). Moreover, it displayed higher inhibitory activity ($EC_{50} = 1.6 \mu M$) against STAT3 than siltitasertib, CX-4945 ($EC_{50} = 5.3 \mu M$).⁶⁶

However, two later studies published by Lindenblatt et al.⁶⁷ and Brear et al.⁶⁸ in 2020 revealed that compound **29** did not bind to the allosteric site of CK2 and instead it performed its inhibitory activity by occupying the ATP cavity. Lindenblatt et al. examined the crystal structure of CK2 α with compound **29** (PDB ID 6TEW) and performed a kinetic study to prove the exact binding mode.⁶⁷ Brear et al.⁶⁸ also reported the crystal structures of CK2 α with compound **29** (PDB ID 6YPG and 6YPH) and performed competitive isothermal titration calorimetry (ITC) and NMR, hydrogen–deuterium exchange (HDX) mass spectrometry, and chemoinformatic analyses. All these experiments showed that the compound occupied the ATP binding site and not an allosteric site.⁶⁸

Figure 19 illustrates the X-ray data of compound **29** bound to CK2 α (PDB ID 6YPG). The carboxylic acid and the OH group formed H-bonds with the amino group of Lys68 and with Asp175. Another water mediated H-bond was seen between the carboxylic group and Glu81 and Trp176. The π –H interaction could be observed between the five-membered ring and Met163 and between the naphthyl group and His160.⁶⁸

In 2019, Oshima et al. identified the guaiacol derivative **30** (Figure 20) as a period-lengthening (circadian clock modulating) compound that inhibited CK2 α with $IC_{50} = 7$ nM.⁶⁹ The compound was identified using the affinity-based proteomics approach. The structure is formed of a triazole ring linked to bromoguaiacol and substituted with methyl thioether and a phenyl moiety. SAR study indicated the importance of triazole and bromoguaiacol rings for the enzyme inhibitory activity. The removal of substituents on the bromoguaiacol ring resulted in a complete loss of activity. Removal of the methyl thioether group or the phenyl moiety retained the inhibitory activity, and modifications could be done at the *para* position of the phenyl group.⁶⁹ The authors determined the X-ray crystal structure of human CK2 α in complex with compound **30** at a resolution of 1.68 Å (Figure 21). The

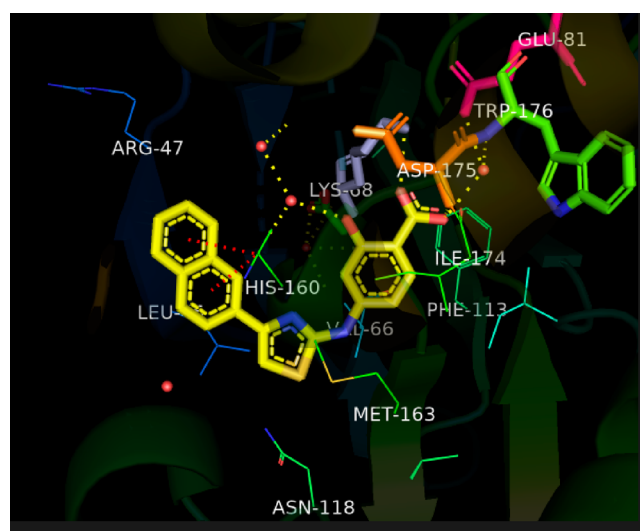


Figure 19. X-ray cocrystal structure of compound **29** with CK2 α (PDB ID 6YPG; 1.51 Å). The figure was generated using PyMOL 2.4.0 with the CK2 α protein shown as a cartoon and compound **29** shown as sticks colored by the atom type: C, yellow; O, red; and N, blue. The H-bonds are illustrated in yellow dashed lines, π – π interaction in red color. The bound water molecules are shown as red spheres.

oxygen atoms in the hydroxy and methoxy groups of bromoguaiacol formed H-bonds with Lys68 from gatekeeper β , whereas the bromine atom of the bromoguaiacol interacted through water mediated H-bonds with the backbone C=O of Glu114 and NH of Val116 at the hinge region. The methyl of the methyl thioether group made hydrophobic interactions with Val66 and Met163 from the top and bottom of the cavity, respectively. The phenyl group made a π – π interaction with His160. The results showed that the compound fit deeply in the ATP binding site at the interface of the N- and C-terminal domains, indicating that the compound is an ATP-competitive inhibitor of CK2 α . However, the X-ray crystal structure of this compound with CK2 α showed no interaction with the hinge region in the ATP binding site.⁶⁹ Compound **30** showed anticancer activity correlated with cellular clock function.⁶⁹

Allosteric Inhibitors. In spite of the potency of ATP-competitive inhibitors, they suffer from off-target side effects owing to their nonselectivity. This drawback can be overcome using allosteric inhibitors.

Allosteric inhibitors bind to a different site adjacent to the ATP active site and thereby inhibit the binding of ATP to the enzyme. Three major CK2 allosteric sites were identified in the literature. These are the α/β interface, the αD pocket, and the interface between the αC helix and the glycine-rich loop.^{70,71}

The α/β interface has a small size (832 Å²) and contains a small binding pocket on the CK2 α side that can be occupied by small molecules. Binding to the α/β interface prevents the assembly of the CK2 tetramer by preventing the association of the β subunit while it preserves the CK2 monomer catalytic activity.^{72,73} Examples of such inhibitors include the ATP-competitive inhibitor DRB (Figure 1) that binds also to the α/β interface,⁷² a peptide named Pc that was derived from the CK2 β carboxy-terminal domain⁷⁴ and its derivatives.^{75,76} However, all these derivatives are not cell permeable except for a derivative named TAT-Pc.⁷⁷ Other small compounds that target the CK2 α /CK2 β interface include CAM187 (Figure 22) with an IC_{50} of 44 μM .⁷⁸

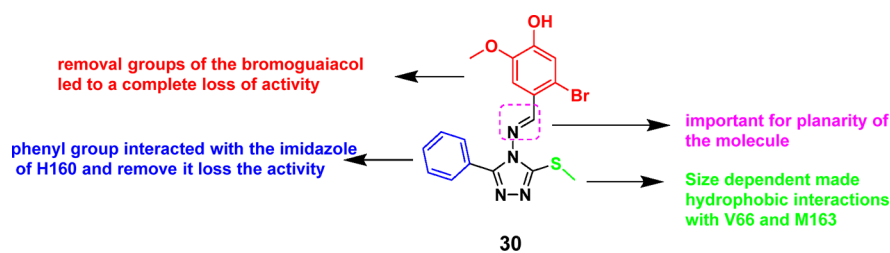


Figure 20. SAR study of compound 30.

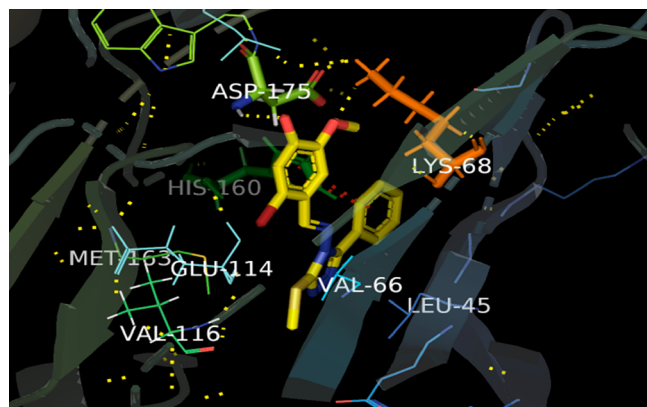


Figure 21. X-ray cocrystal structure of compound 30 with CK2 α (PDB ID 6A1C; 1.68 Å). The figure was generated using PyMOL 2.4.0 with the CK2 α protein shown as a cartoon and compound 30 shown as sticks colored by the atom type: C, yellow; O, red; N, blue; and Br, magenta. The H-bonds are illustrated in yellow dashed lines.

Examples of inhibitors that bind to the α D pocket include CAM4066 ($IC_{50} = 0.370 \mu\text{M}$) and CAM4712 ($IC_{50} = 7 \mu\text{M}$) (Figure 22).^{79–81}

The main drawback of this type of inhibitor is their poor cell permeability. This problem can be solved by the preparation of a prodrug that can cross the cell membrane and then hydrolyze inside the cell to release the active drug.⁸²

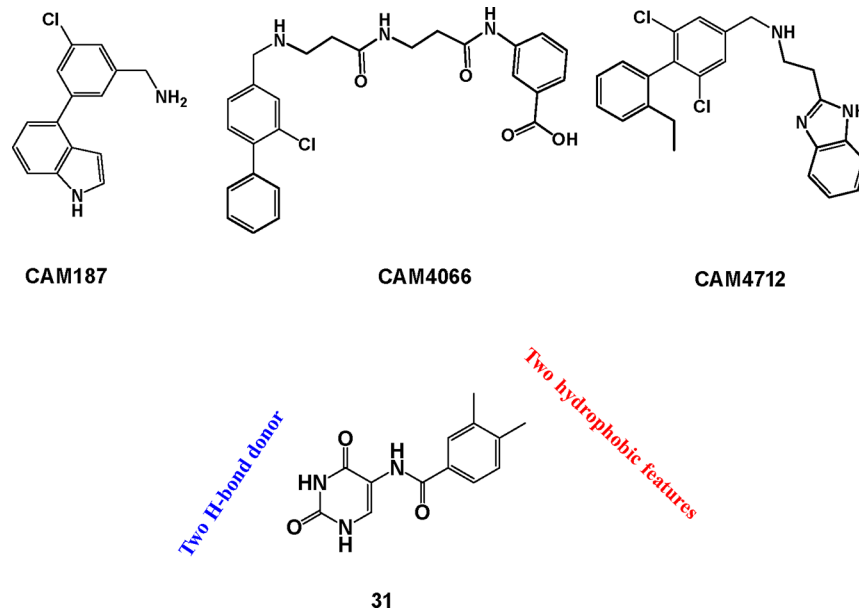


Figure 22. Structures of CK2 allosteric inhibitors.

In 2020, Li et al.⁸³ used the structural based pharmacophore modeling and Alloscore website for screening the ChemBridge fragment library to identify the potent allosteric CK2 inhibitor, 31 (Figure 22). The latter displayed non-ATP-competitive CK2 inhibition ($IC_{50} = 13.0 \mu\text{M}$) with noticeable antiproliferative activity on A549 cancer cells ($IC_{50} = 23.1 \mu\text{M}$). The MD simulation results indicated that the compound skeleton occupied the α D pocket and the uracil formed polar interactions with Val162 and Asn118. Additionally, the NH linker bound with Val162 and Pro159 as well as the phenyl ring buried in the hydrophobic pocket formed by Tyr136, Ile133, Met221, and Met225 (Figure 23).⁸³

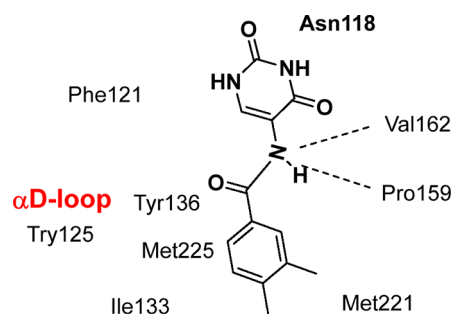


Figure 23. Interactions of compound 31 with residues in CK2 α active site.

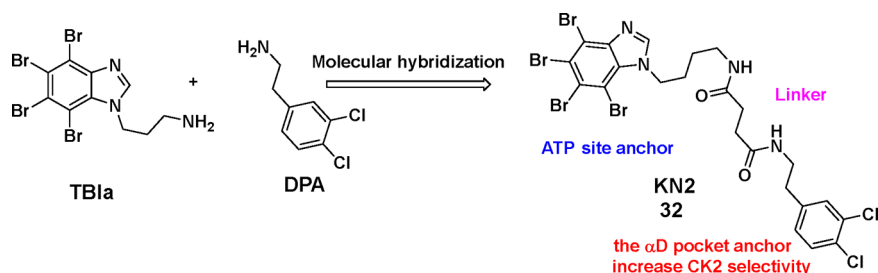


Figure 24. Design of compound 32.

In an attempt to prepare a selective CK2, the α D pocket of CK2 α was targeted by linking 4-(4,5,6,7-tetrabromo-1H-benzo[*d*]-imidazol-1-yl)butan-1-amine (TBIa) and 3,4-dichlorophenethylamine (DPA) using a tailor-made linker. TBIa is a potent ATP-competitive inhibitor but has low selectivity, while DPA has high selectivity toward the α D pocket but with low affinity. The design of the linker was based upon the atomic resolution of the CK2 α' structure in complex with an ATP site and an α D pocket fragment. These efforts resulted in the identification of the bivalent compound KN2 (compound 32, Figure 24) with IC_{50} values of 19.3 ± 6.4 nM and 15.6 ± 5.5 nM for the CK2 $\alpha 2\beta 2$ and the CK2 $\alpha' 2\beta 2$ isoforms, respectively. The kinase profiling of this compound proved its high selectivity for CK2.⁸⁴

Figure 25 illustrates the binding of KN2 (32) to the CK2 active site. The four bromine atoms participated via two

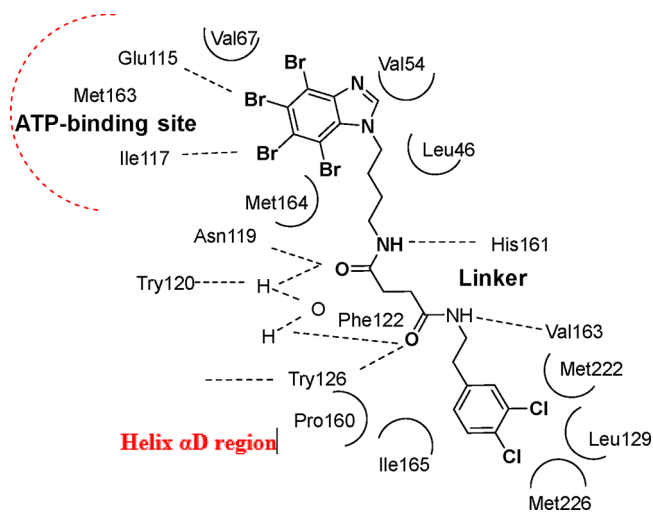


Figure 25. Main interactions of compound 32 in CK2 pocket.

halogen bonds with Glu115 and Ile117 in the hinge region and via hydrophobic interactions with Val67, Met164, and Ile175.

Other hydrophobic interactions were observed with Phe122, Try125, and Ile140. The two carbonyl groups of the linker made two H-bonds with Asn119 and Try126, while the two amino groups of the linker shared two H-bonds with His161 and Val163. Finally, the dichlorophenyl ring was buried in the α D pocket and surrounded by hydrophobic residue Ile165, Met226, Leu126, and Met222.

The tetrabromo benzimidazole ARC-1502 (compound 33, Figure 26) was a bisubstrate inhibitor with a K_i value of 0.56 nM that bound to the CK2 α /CK2 β interface. Its structure consisted of an ATP-competitive head and a peptide tail linked by a specific linker to enable the peptide to fill a substrate cleft in the CK2 catalytic subunit.⁸² In 2020, Pietsch et al.⁸⁵ reported the preparation of its isostere tetraiodobenzimidazole ARC-3140 (compound 34, Figure 26) that exhibited an extraordinary affinity to the CK2 enzyme with a K_i value of 84 nM. This derivative bound to both the ATP binding site and the substrate binding site, probably the CK2 β interface of CK2 α . The incorporation of an amide linkage not only enhanced the affinity for the enzyme but also enhanced the cell permeability of the compound, a problem that accounted for the poor cellular activity of most CK2 inhibitors.⁸⁵

Kufareva et al. used the interface fumigation modeling protocol followed by druggable pocket selection and virtual screening to identify the exosite lead compound 35 (CK2, $IC_{50} = 50$ μ M) that can bind to the CK2 α /CK2 β interface. Further development and SAR studies were done to identify novel CK2 inhibitors that act selectively on the CK2 α /CK2 β interface.⁸⁶ This study explored some structural modifications including the removal of the 2-methoxy group and 5-fluorine atom of the indole ring, as well as the replacing the methylsulfonamide with a phenylsulfonamide group to afford the compound 36 ($IC_{50} = 45$ μ M) and the most active compound 37 ($IC_{50} = 22$ μ M) (Figure 27). Compound 37 induced apoptosis in breast cancer cells (MBA-MB-231) with good cell permeability. The crystal structures of 36 and 37 demonstrated that they bound at the CK2 α /CK2 β interface, which accounted for the specific inhibition of CK2 β dependent substrates. In addition, they showed allosteric effects that

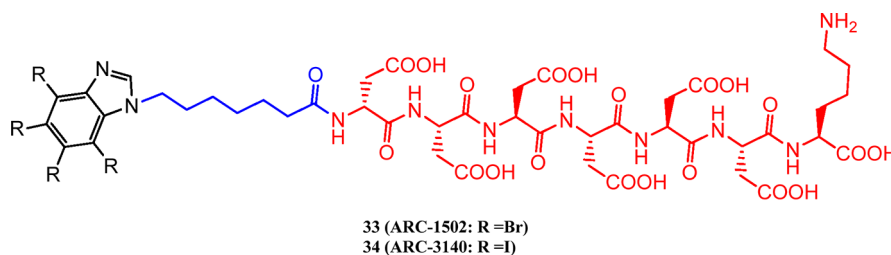


Figure 26. Structure of compounds 33 and 34.

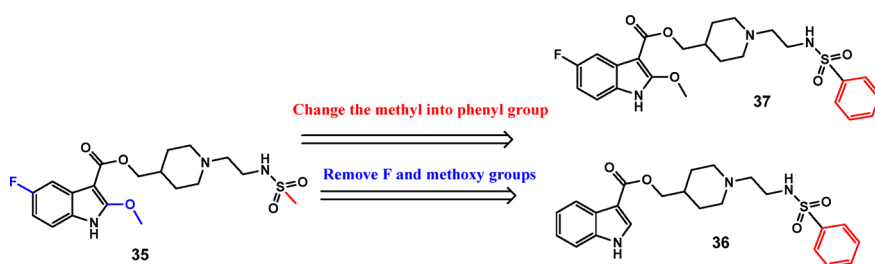


Figure 27. Design of compounds 36 and 37.

caused the transition of the α D loop from the open to the closed conformation. Moreover, the fluorinated indole ring in compound 37 was buried in the hydrophobic part of the binding pocket formed by Ala110, Leu41, Ile69, Val67, Val101, Val105, Val112, and Pro104 (Figure 28). In addition, the

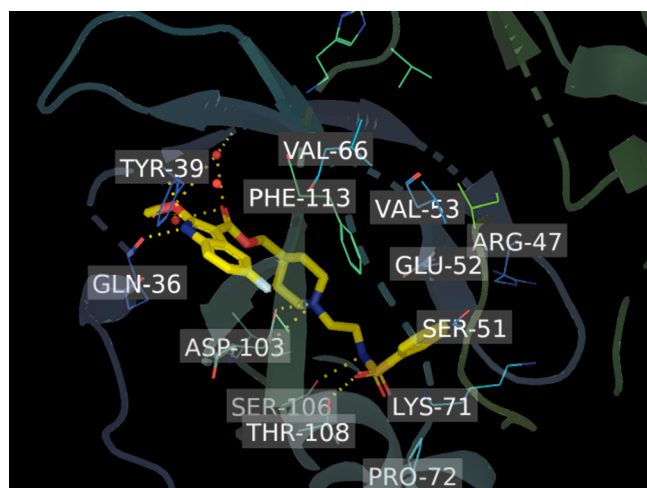


Figure 28. X-ray cocrystal structure of compound 37 with CK2 α (PDB ID 6FVF; 1.47 Å). The figure was generated using PyMOL 2.4.0 with the CK2 α protein shown as a cartoon and compound 37 shown as sticks colored by the atom type: C, yellow; O, red; and N, blue. The H-bonds are illustrated in yellow dashed lines. The bound water molecules are shown as red spheres.

methoxy ether oxygen and the NH of the indole ring form polar interactions with Tyr39 and Gln36. Furthermore, the carbonyl of the Asp103 kinase P-loop formed a salt bridge interaction with the nitrogen of piperidine. Additionally, the amino group of phenylsulfonamide was engaged by a direct hydrogen bond with Ser106, while carbonyls of sulfonamide formed hydrogen bonds with the amino acid residue Thr108

and Pro72 of the β 4– β 5 loop. Meanwhile, the phenyl group occupied the shallow pocket formed by Arg47, Glu52, and Lys71.⁸⁶

Dual Inhibitors or Multitarget Inhibitors. This type of inhibitor is formed of two conjugated or hybridized compounds that can affect two or more enzymes inside the body. This strategy avoids the use of two drugs and could overcome the resistance developed against one of the drugs. This can be exemplified by the work done by Martinez et al., who prepared conjugated molecules of TBB or DMAT and a zinc binding group.⁸⁷ The authors applied a pharmacophoric hybridization strategy of DMAT (CK2 inhibitor, IC₅₀ = 0.14 μ M) and SAHA (HDAC1 inhibitor, IC₅₀ = 10 nM) to prepare dual CK2/HDAC inhibitors (Figure 29). Compound 38 was the most active among this series as an HDAC1 (IC₅₀ = 1.46 μ M), HDAC6 (IC₅₀ = 0.66 μ M), and CK2 (IC₅₀ = 3.67 μ M) inhibitor and exhibited promising antiproliferative activity against Jurkat, MCF-7, HCT-116, and HL-60 cell lines.⁸⁷

The pharmacophoric hybridization and linker chain extension strategies of the CK2 inhibitor CX-4945 and the hydroxamic acid of HDAC1 inhibitor SAHA led to the development of new dual CK2/HDAC1 inhibitors (Figure 30). The most potent inhibitor was compound 39, in which the seven-carbon linker was important for balanced and optimal inhibition of both HDAC1 and CK2. Remarkably, compound 39 showed higher activity than SAHA (HDAC1) and CX-4945 (CK2) by 3.5 and 3.0 times, respectively. Compound 39 showed micromolar activity in cell-based cytotoxic assays against PC3, LNCaP, and MCF-7 cell lines.⁸⁸

Similarly, the conjugation of cisplatin and CK2 inhibitor (CX-4945) resulted in a compound with promising antitumor activity *in vitro* and *in vivo* that can overcome the resistance developed versus cisplatin and reduce the side effects of cisplatin and related platinum drugs.^{89,90} In 2020, Chen et al. reported the preparation of two conjugated platinum prodrugs named Cx-platin-Cl and Cx-DN604-Cl (Figure 31).⁸⁹ The *in vitro* and *in vivo* studies revealed that both prodrugs were

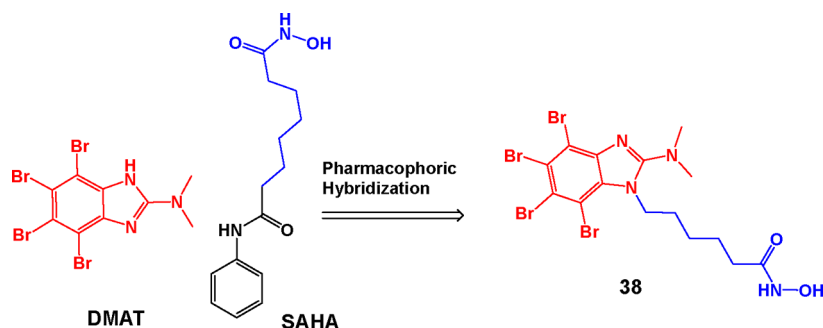


Figure 29. Design of dual HDAC/CK2 inhibitor 38.

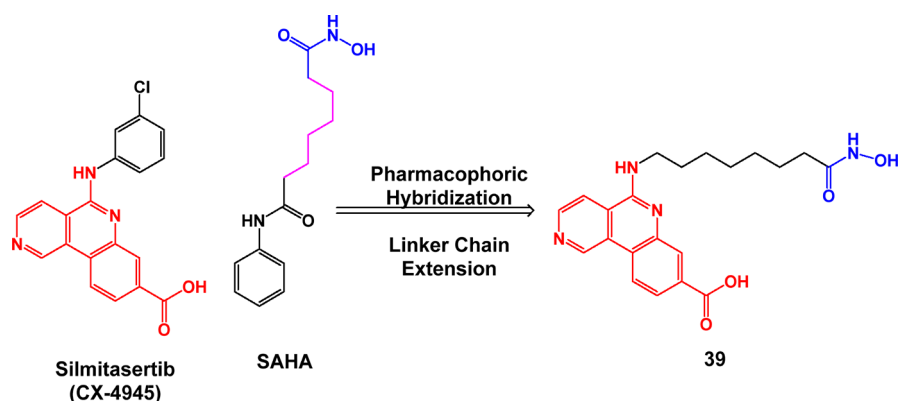


Figure 30. Design of dual HDAC/CK2 inhibitor 39.

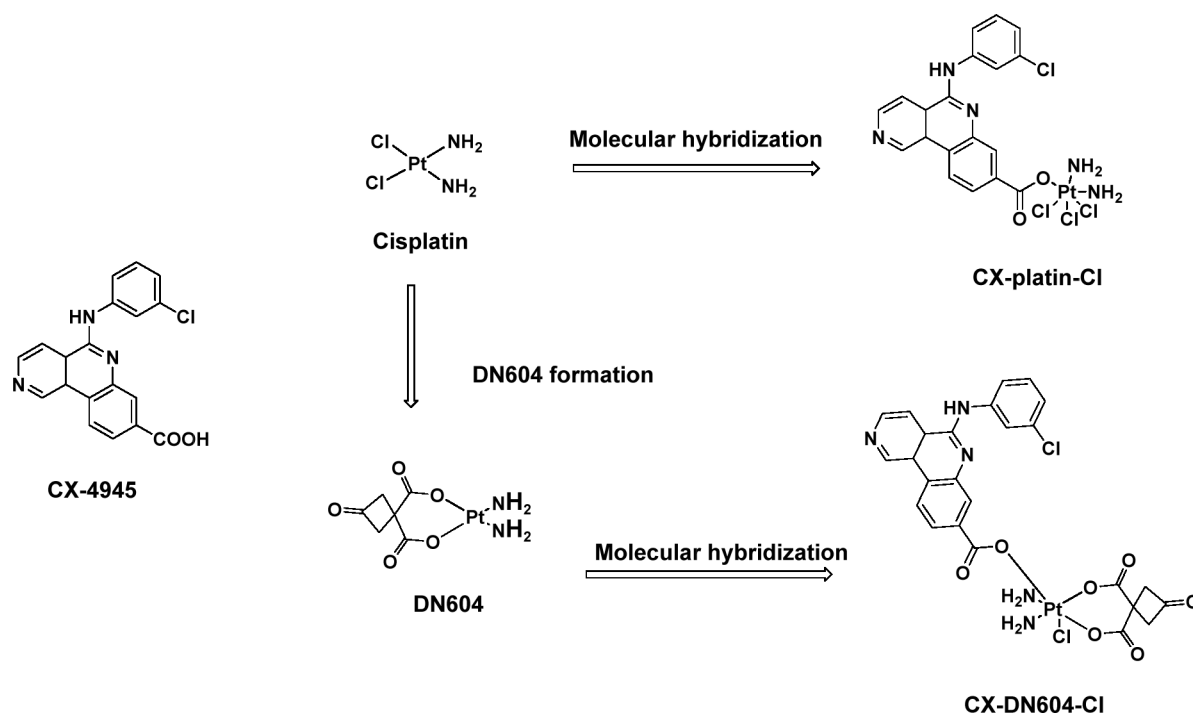


Figure 31. Design of cisplatin and CK2 inhibitor conjugate.

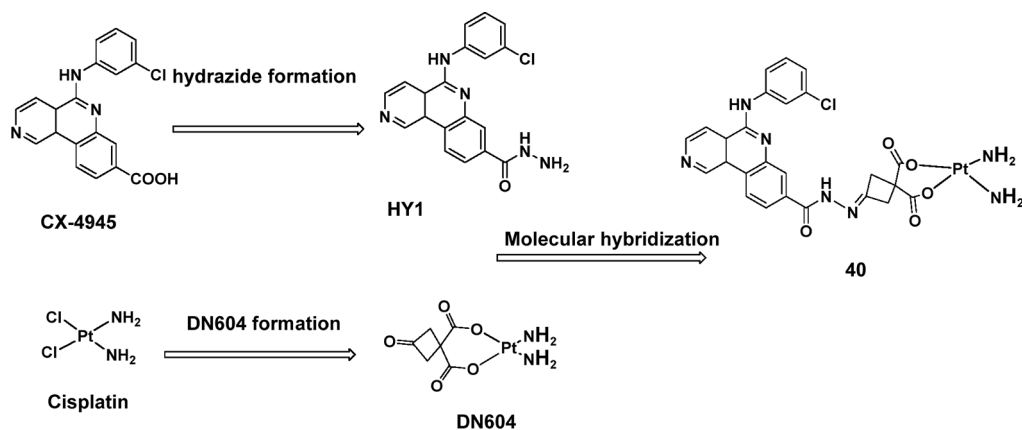


Figure 32. Design of cisplatin and CK2 inhibitor conjugate 40.

superior to cisplatin and DN604 in suppressing cancer cell growth. They exerted their antitumor effects through suppression of JWA-XRCC1 mediated single-strand-break

repair. The JWA gene is activated in response to DNA damage, and it has a vital role in cell differentiation. However,

improper DNA repair may trigger tumor cells. Therefore, suppression of this gene inhibits the formation of tumor cells.⁸⁹

One year later, a hydrazide derivative (HY1) of CX-4945 was developed by the same research group to enhance the antitumor efficacy and overcome the cisplatin-induced resistance in A549/cDDP cells.⁹⁰ The new compound, **40** (Figure 32), was developed by molecular hybridization of HY1 and an active Pt(II) derivative. Derivative **40** (HY1-Pt) exhibited cytotoxicity nearly as potent as cisplatin in A549 cells and strong inhibitory activity against these cancer cells, especially cisplatin mediated drug-resistant cancer cells.⁹⁰ Compound **40** also arrested the cell cycle in the S phase; similar to cisplatin. Meanwhile, both A549 and A549/cDDP cells were highly sensitive to compound **40** with apoptotic percentages from 66.9 to 85.5% compared to cisplatin, which showed apoptotic percentages from 46.1 to 19.2%. The compound exerted this action by inhibition of CK2, enhancing cellular accumulation of platinum and inhibition of DNA repair.⁹⁰

Recently, in 2021, Wang and his group reported structure modification of sunitinib (CX-4945) to increase the CK2 selectivity, improve the physicochemical properties, and enhance the anticancer activity especially on cancer stem cells (CSCs).⁹¹ The modification was done by replacing the carboxylic group in CX-4945 with the bioisosteric amidic group that can act as an H-bond donor and/or acceptor similar to the carboxylic group. Their efforts resulted in the identification of compound **41** (Figure 33) containing a 2-

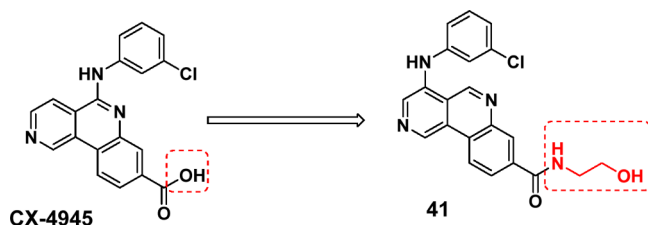


Figure 33. Design of dual Clk2/CK2 inhibitor **41**.

hydroxyethyl side chain attached to the CX-4945 scaffold. The inhibitory activity of compound **41** against CK2 was 0.66 nM with a high selectivity for Clk2/CK2 (142 times higher than that of CX-4945). This can overcome the off-target side effects of CX-4945.⁹¹ Furthermore, compound **41** exhibited potent antiproliferative activities against five different CK2-overexpressed cancer cells as well as cancer stem cells. The effect on CSCs was attributed to the ability of compound **41** to inhibit the Akt1(ser129)-GSK-3 β (ser9)-Wnt/ β -catenin signaling

pathway and inhibit the expression of the stemness marker ALDH1A1, CSC surface antigens (CD44+ and CD133+), and stem genes (SOX2, OCT4, and Nanog). The pharmacokinetic properties of compound **41** were far better than those of CX-4945 sodium salt with no toxicity.⁹¹

The docking study indicated that the binding mode of compound **41** to CK2 was achieved through the amide group that formed two H-bonds with Trp175 and Thr112 residues. The nitrogen atom on ring A of naphthyridine formed an H-bond with the Val115 residue. Meanwhile, the hydroxyl group on the side chain of 2-aminoethanol formed hydrogen bonds with Asp174 and Glu80 residues. These five hydrogen bonds enabled compound **41** to be deeply and firmly anchored in the CK2 α active cavity (Figure 34a). On the other hand, the binding mode of compound **41** to the Clk2 pocket was achieved via only three hydrogen bonds between compound **41** and the amino acid residues Asp127 and Glu224 (Figure 34b). Therefore, compound **41** was not inserted deep into the activity cavity of Clk2.

A novel dual inhibitor of bromodomain containing protein 4 (BRD4) and CK2 was developed by Zhang et al. in 2021.⁹² The quinazoline lead compound **42** (Figure 35) was optimized through rational drug design, SAR, and *in vivo* and *in vitro* biological evaluations to generate the BRD4/CK2 dual inhibitor, **43** (Figure 35). Compound **43** showed excellent inhibitory activity against CK2 (90.65%) and BRD4 (92.28%) with an antiproliferative effect on MDA-MB-231 (IC_{50} = 2.66 μ M) and MDA-MB-468 (IC_{50} = 3.52 μ M) cells. In addition, it induced apoptotic and autophagy-associated cell death for triple-negative breast cancer therapy (TNBC). Moreover, it showed accepted pharmacokinetic properties and low toxicity and can be used in the treatment of TNBC.⁹²

Chojnacki et al.⁹³ explored the new aminoalkyl-substituted derivatives **44** and **45** (Figure 36) via the optimization of CK2 inhibitor 4,5,6,7-tetrabromo-1*H*-benzimidazole (TBBi). This optimization involved the introduction of an aminopropyl group and/or a C2-methyl group to afford new dual CK2 α /PIM1 kinase inhibitors, **44** and **45**. They inhibited CK2 with IC_{50} = 0.37 and 0.36 μ M, respectively, and inhibited PIM1 with IC_{50} = 33 and 0.17 μ M, respectively. These compounds showed good antiproliferative activities against MCF-7, CCRF-CEM, and PC-3 human cancer cell lines. The binding mode of **44** with CK2 α' (PDB ID 3OFM) revealed that three halogen bonds were formed between Br(C7), Br(C6), and Br(C4) and the oxygen of Asn118, the carbonyl oxygen of Val116, and the aromatic side chain of Phe113. In addition, a hydrogen bond was formed between the amino group and His160, while the protonated amino propyl group was ionically bonded to

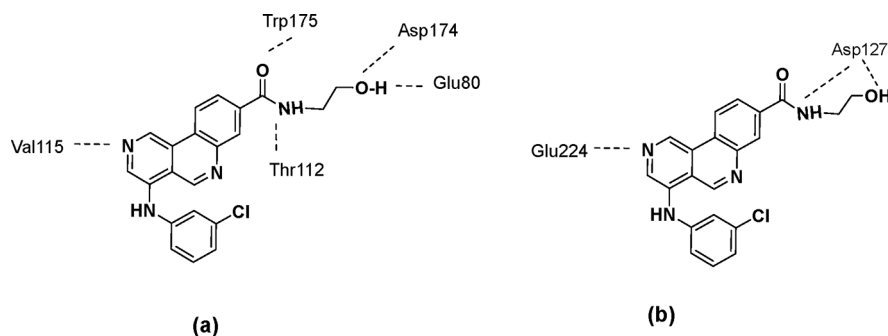


Figure 34. (a) The main interactions of compound **41** in CK2 pocket. (b) The main interactions of compound **41** in Clk2 pocket.

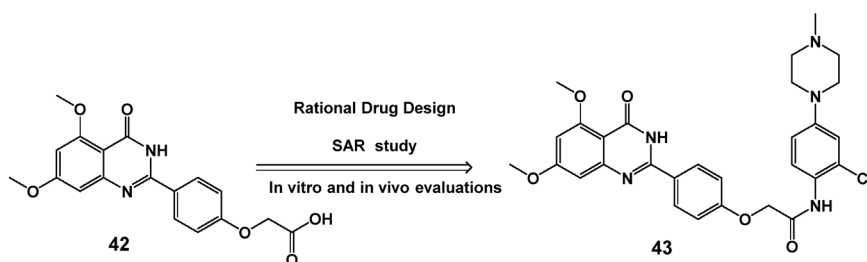


Figure 35. Design of dual BRD4/CK2 inhibitor 43.

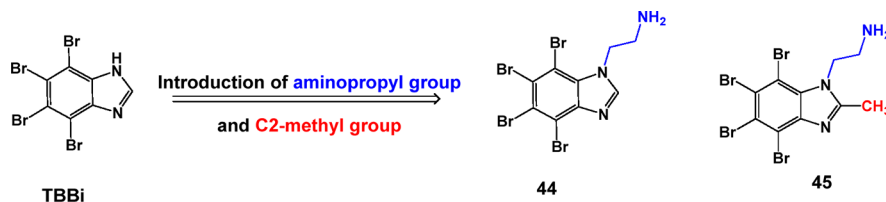


Figure 36. Design of dual PIM1/CK2 α inhibitors 44 and 45.

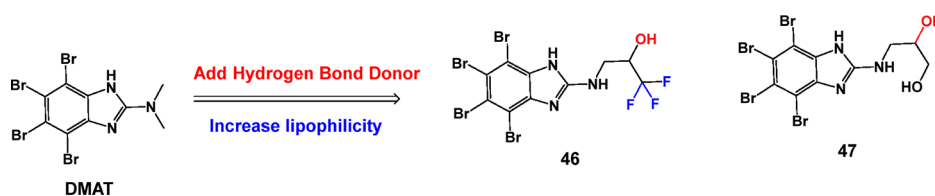


Figure 37. Design of dual PIM1/CK2 α inhibitors 46 and 47.

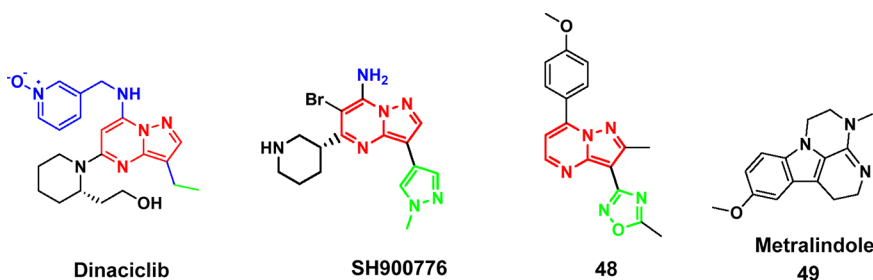


Figure 38. Structures of multikinase inhibitor 48 and the dual CDK2/CK2 inhibitor 49.

Asp120. The binding of compound 44 maintain closed conformation of the hinge/helix α D region.⁹³

In 2023, Wińska and co-workers discovered novel aminoalcohol derivatives of parental DMAT as potent dual CK2/PIM-1 inhibitors (Figure 37).⁹⁴ This effort concentrated on the introduction of aliphatic aminoalcohol substituents to the lead structure DMAT to afford compounds 46 and 47, which displayed high binding affinities to CK2 and PIM-1 enzymes. Compounds 46 and 47 inhibited CK2 with K_i values of 0.294 and 0.151 μ M, respectively, and inhibited PIM1 with K_i values of 0.067 and 0.073 μ M, respectively. Moreover, compound 46 showed good inhibition against acute lymphoblastic leukemia cells and induced apoptosis. Meanwhile, compound 47 induced apoptosis in breast cancer cells.⁹⁴

Recently, in 2023, Al-Qadhi et al. used proper substitution and insertion strategies around pyrazolo[1,5-*a*]pyrimidine scaffold to develop multitarget kinase inhibitors.⁹⁵ The rationale of this work was based on the structures of the CDK2 and CHK1 inhibitors Dinaciclib and SCH900776. The pyrazolo[1,5-*a*]pyrimidine core was kept as a hinge binding moiety to take the place of adenine in the ATP binding pocket;

then structural modifications were carried out around this scaffold by the proper selection of different pharmacophoric substituents at position 3 (carbonitrile, carboxamide, amidoxime, and 1,2,4-oxadiazole). Additionally, different aryl substituents were introduced at position 7 to occupy the hydrophobic pocket and to augment the hydrophobic interactions around the hinge region.⁹⁵ The most active compound on CK2 α was the oxadiazole derivative 48 (Figure 38) with $IC_{50} = 0.093 \mu$ M. This compound also showed high inhibitory activity on TrkA, ALK2, c-KIT, EGFR, PIM1, CHK1, and CDK2 in submicromolar concentrations. Compound 10e exhibited antitumor activity against MCF7, HCT116, and EK VX cell lines and arrested the cell cycle in the G1/S phase and G1 phase in MCF7 and HCT116 cells.⁹⁵

In 2023, Al-Dhuayan and ALaqeel identified Metralindole 49 (Figure 38) as a CDK2 and CK2 inhibitor through molecular docking, ADMET, and molecular dynamics simulation of the DrugBank prepared library. The binding mode of Metralindole 49 in the active pockets of CDK2 and CK2 displayed good docking scores and bonding topologies. The binding mode of compound 49 with CK2 revealed that

one H-bond was formed between the oxygen atom of the methoxy group of Lys68. Additionally, π - π stacking interaction between the phenyl ring and Phe113 was observed. On the other hand, the results of ADMET studies of Metralindole **49** showed excellent bioavailability, outstanding solubility, and high safety. These facts encouraged the use of Metralindole as an effective candidate in the treatment of lung cancer.⁹⁶

CONCLUSION AND FUTURE PROSPECTIVE

The CK2 enzyme has a vital role in controlling many processes inside the body in addition to its ability to phosphorylate over 400 substrates. This initiated the need for the development of CK2 inhibitors to control many diseases, including cancer and CNS diseases. In spite of the efforts done in this field for more than two decades, only two compounds entered clinical trials to treat cancer.

The design of the ATP-competitive type I inhibitors relied on three common pharmacophoric features: the heterocyclic ring system bearing one or two hydrogen bond donors or acceptors that occupied the purine binding site, the head carrying hydrophilic substituents extended in the solvent exposed area, and the tail occupying the neighboring hydrophobic regions which control the binding potency and affinity. A 3D-QSAR and molecular docking studies on 2,4,5-trisubstituted imidazole was recently reported by Goudzal et al. in 2023. The study was performed on 24 compounds, and the authors developed a reliable model for the prediction of enzyme inhibitory and anticancer activity.⁹⁷ Another pharmacophoric model was developed by Yadav et al. in 2023 to design CK2 inhibitors as a treatment for COVID-19.⁹⁸ The design was inspired by the structure of silitasertib. Several strategies were applied in this study, including bioisosteric replacement and molecular docking. Then, ligand-based pharmacophore models and structure-based pharmacophores (e-pharmacophores) were utilized to build a hybrid hypothesis. The latter include three chemical features, namely an anion, an aromatic ring, and an H-bond acceptor.⁹⁸ A similar model was developed by Patel et al. using both structure- and fragment-based design strategies. The structure-based pharmacophore hypothesis suggested by the authors relied on four features ARRR: an H-bond acceptor (A) and three aromatic rings (RRR).⁹⁹ The design of these models might help the researcher in the design of more selective ATP-competitive CK2 inhibitors.

The poor cellular activity of most CK2 inhibitors originated from their poor cell permeability. This could be overcome through the development of allosteric or bisubstrate inhibitors that carried lipophilic groups. The allosteric inhibitors are more selective to CK2 and hence could overcome the off-target side effects of ATP-competitive inhibitors that are nonselective. Another successful strategy to attain cellular activity is the preparation of dual inhibitors that target other enzyme or molecular hybridization with a well-known anticancer drug like cisplatin. Further studies are still needed in order to discover a clinically potent CK2 inhibitor.

AUTHOR INFORMATION

Corresponding Author

Mustafa A. Al-Qadhi – Department of Medicinal Chemistry, Faculty of Pharmacy, Sana'a University, 18084 Sana'a, Yemen; Email: m777329509@gmail.com, mustafa.alqadhi@std.pharma.cu.edu.eg

Authors

Tawfeek A. A. Yahya – Department of Medicinal Chemistry, Faculty of Pharmacy, Sana'a University, 18084 Sana'a, Yemen

Hala B. El-Nassan – Pharmaceutical Organic Chemistry Department, Faculty of Pharmacy, Cairo University, Cairo 11562, Egypt; orcid.org/0000-0001-9904-1264

Complete contact information is available at:

<https://pubs.acs.org/10.1021/acsomega.3c10478>

Notes

The authors declare no competing financial interest.

REFERENCES

- (1) Meggio, F.; Pinna, L. A. One-thousand-and-one Substrates of Protein Kinase CK2? *FASEB J.* **2003**, *17* (3), 349–368.
- (2) Franchin, C.; Borgo, C.; Zaramella, S.; Cesaro, L.; Arrigoni, G.; Salvi, M.; Pinna, L. A. Exploring the CK2 Paradox: Restless, Dangerous, Dispensable. *Pharmaceuticals* **2017**, *10* (1), 11.
- (3) Niefind, K.; Guerra, B.; Pinna, L. A.; Issinger, O. G.; Schomburg, D. Crystal Structure of the Catalytic Subunit of Protein Kinase CK2 from *Zea Mays* at 2.1 Å Resolution. *EMBO J.* **1998**, *17* (9), 2451–2462.
- (4) Poletto, G.; Vilardell, J.; Marin, O.; Pagano, M. A.; Cozza, G.; Sarno, S.; Itarte, E.; Pinna, L. A.; Meggio, F.; Falques, A. The Regulatory Subunit of Protein Kinase CK2 Contributes to the Recognition of the Substrate Consensus Sequence. A Study with an EIF2-Derived Peptide. *Biochemistry* **2008**, *47*, 8317–8325.
- (5) Franchin, C.; Borgo, C.; Cesaro, L.; Zaramella, S.; Vilardell, J.; Salvi, M.; Arrigoni, G.; Pinna, L. A. Re-Evaluation of Protein Kinase CK2 Pleiotropy: New Insights Provided by a Phosphoproteomics Analysis of CK2 Knockout Cells. *Cell. Mol. Life Sci.* **2018**, *75* (11), 2011–2026.
- (6) Niefind, K.; Pütter, M.; Guerra, B.; Issinger, O.-G.; Schomburg, D. GTP plus Water Mimic ATP in the Active Site of Protein Kinase CK2. *Nat. Struct. Biol.* **1999**, *6* (12), 1100–1103.
- (7) Issinger, O. CASEIN KINASES: PLEIOTROPIC MEDIATORS OF CELLULAR REGULATION. *Pharmac. Ther.* **1993**, *59*, 1–30.
- (8) Allende, J. E.; Allende, C. C. Protein Kinase CK2: An Enzyme with Multiple Substrates and a Puzzling Regulation. *FASEB J.* **1995**, *9*, 313–323.
- (9) Sarno, S.; Ghisellini, P.; Pinna, L. A. Unique Activation Mechanism of Protein Kinase CK2. *J. Biol. Chem.* **2002**, *277* (25), 22509–22514.
- (10) Sarno, S.; Vaglio, P.; Meggio, F.; Issinger, O.; Pinna, L. A. Protein Kinase CK2 Mutants Defective in Substrate Recognition. *J. Biol. Chem.* **1996**, *271* (18), 10595–10601.
- (11) Manni, S.; Brancalion, A.; Mandato, E.; Tubi, L. Q.; Colpo, A.; Pizzi, M.; Cappellesso, R.; Zaffino, F.; Di Maggio, S. A.; Cabrelle, A.; et al. Protein Kinase CK2 Inhibition Down Modulates the NF-KB and STAT3 Survival Pathways, Enhances the Cellular Proteotoxic Stress and Synergistically Boosts the Cytotoxic Effect of Bortezomib on Multiple Myeloma and Mantle Cell Lymphoma Cells. *PLoS One* **2013**, *8* (9), No. e75280.
- (12) Ruzzene, M.; Bertacchini, J.; Toker, A.; Marmiroli, S. Cross-Talk between the CK2 and AKT Signaling Pathways in Cancer. *Adv. Biol. Regul.* **2017**, *64*, 1–8.
- (13) Trembley, J. H.; Chen, Z.; Unger, G.; Slaton, J.; Kren, B. T.; Van Waes, C.; Ahmed, K. Emergence of Protein Kinase CK2 as a Key Target in Cancer Therapy. *BioFactors* **2010**, *36* (3), 187–195.
- (14) de Gooijer, M. C.; Guillén Navarro, M.; Bernards, R.; Wurdinger, T.; van Tellingen, O. An Experimenter's Guide to Glioblastoma Invasion Pathways. *Trends Mol. Med.* **2018**, *24* (9), 763–780.
- (15) Duncan, J. S.; Turowec, J. P.; Vilk, G.; Li, S. S. C.; Gloor, G. B.; Litchfield, D. W. Regulation of Cell Proliferation and Survival:

- Convergence of Protein Kinases and Caspases. *Biochim. Biophys. Acta - Proteins Proteomics* **2010**, *1804* (3), 505–510.
- (16) Scaglioni, P. P.; Yung, T. M.; Choi, S.; Baldini, C.; Konstantinidou, G.; Pandolfi, P. P. CK2 Mediates Phosphorylation and Ubiquitin-Mediated Degradation of the PML Tumor Suppressor. *Mol. Cell. Biochem.* **2009**, *327* (1–2), 279.
- (17) Guerra, B.; Issinger, O. Protein Kinase CK2 in Human Diseases. *Curr. Med. Chem.* **2008**, *15* (19), 1870–1886.
- (18) Gowda, C.; Sachdev, M.; Muthisami, S.; Kapadia, M.; Petrovic-Dovat, L.; Hartman, M.; Ding, Y.; Song, C.; Payne, J.; Tan, B.-H.; et al. Casein Kinase II (CK2) as a Therapeutic Target for Hematological Malignancies. *Curr. Pharm. Des.* **2017**, *23* (1), 95–107.
- (19) Ruzzene, M.; Pinna, L. A. Addiction to Protein Kinase CK2: A Common Denominator of Diverse Cancer Cells? *Biochim. Biophys. Acta - Proteins Proteomics* **2010**, *1804* (3), 499–504.
- (20) Borgo, C.; Ruzzene, M. Role of Protein Kinase CK2 in Antitumor Drug Resistance. *J. Exp. Clin. Cancer Res.* **2019**, *38* (1), 287.
- (21) Chua, M. M. J.; Ortega, C. E.; Sheikh, A.; Lee, M.; Abdur-Rassoul, H.; Hartshorn, K. L.; Dominguez, I. CK2 in Cancer: Cellular and Biochemical Mechanisms and Potential Therapeutic Target. *Pharmaceuticals* **2017**, *10* (1), 18.
- (22) Di Maira, G.; Gentilini, A.; Pastore, M.; Caligiuri, A.; Piombanti, B.; Raggi, C.; Rovida, E.; Lewinska, M.; Andersen, J. B.; Borgo, C.; et al. The Protein Kinase CK2 Contributes to the Malignant Phenotype of Cholangiocarcinoma Cells. *Oncogenesis* **2019**, *8* (11), 61.
- (23) Lian, H.; Su, M.; Zhu, Y.; Zhou, Y.; Soomro, S. H.; Fu, H. Protein Kinase CK2, a Potential Therapeutic Target in Carcinoma Management. *Asian Pacific J. Cancer Prev.* **2019**, *20* (1), 23–32.
- (24) Buontempo, F.; McCubrey, J. A.; Orsini, E.; Ruzzene, M.; Cappellini, A.; Lonetti, A.; Evangelisti, C.; Chiarini, F.; Evangelisti, C.; Barata, J. T.; et al. Therapeutic Targeting of CK2 in Acute and Chronic Leukemias. *Leukemia* **2018**, *32* (1), 1–10.
- (25) Benavent Acero, F.; Capobianco, C. S.; Garona, J.; Cirigliano, S. M.; Perera, Y.; Urtreger, A. J.; Perea, S. E.; Alonso, D. F.; Farina, H. G. CIGB-300, an Anti-CK2 Peptide, Inhibits Angiogenesis, Tumor Cell Invasion and Metastasis in Lung Cancer Models. *Lung Cancer* **2017**, *107*, 14–21.
- (26) St-Denis, N. A.; Litchfield, D. W. From Birth to Death: The Role of Protein Kinase CK2 in the Regulation of Cell Proliferation and Survival. *Cell. Mol. Life Sci.* **2009**, *66* (11–12), 1817–1829.
- (27) Castello, J.; Ragnauth, A.; Friedman, E.; Rebolz, H. CK2—an Emerging Target for Neurological and Psychiatric Disorders. *Pharmaceuticals* **2017**, *10* (1), 7.
- (28) Perez, D. I.; Gil, C.; Martinez, A. Protein Kinases CK1 and CK2 as New Targets for Neurodegenerative Diseases. *Med. Res. Rev.* **2011**, *31*, 924–954.
- (29) Siddiqui-Jain, A.; Drygin, D.; Streiner, N.; Chua, P.; Pierre, F.; O'Brien, S. E.; Bliesath, J.; Omori, M.; Huser, N.; Ho, C.; et al. CX-4945, an Orally Bioavailable Selective Inhibitor of Protein Kinase CK2, Inhibits Prosurvival and Angiogenic Signaling and Exhibits Antitumor Efficacy. *Cancer Res.* **2010**, *70* (24), 10288–10298.
- (30) Battistutta, R.; Cozza, G.; Pierre, F.; Papinutto, E.; Lolli, G.; Sarno, S.; O'Brien, S. E.; Siddiqui-Jain, A.; Haddach, M.; Anderes, K.; et al. Unprecedented Selectivity and Structural Determinants of a New Class of Protein Kinase CK2 Inhibitors in Clinical Trials for the Treatment of Cancer. *Biochemistry* **2011**, *50* (39), 8478–8488.
- (31) Pierre, F.; Chua, P. C.; O'Brien, S. E.; Siddiqui-Jain, A.; Bourbon, P.; Haddach, M.; Michaux, J.; Nagasawa, J.; Schwaebe, M. K.; Stefan, E.; et al. Discovery and SAR of 5-(3-Chlorophenylamino)-Benzo[c][2,6]Naphthyridine-8-Carboxylic Acid (CX-4945), the First Clinical Stage Inhibitor of Protein Kinase CK2 for the Treatment of Cancer. *J. Med. Chem.* **2011**, *54* (2), 635–654.
- (32) CX-4945 Granted Orphan Drug Designation. *Oncol. Times* **2017**, *39* (5), 23.
- (33) Padgett, C. S.; Lim, J. K. C.; Marschke, R. F.; Northfelt, D. W.; Andreopoulou, E.; Von Hoff, D. D.; Anderes, K.; Ryckman, D. M.; Chen, T. K.; O'Brien, S. E. 414 Clinical Pharmacokinetics and Pharmacodynamics of CX-4945, a Novel Inhibitor of Protein Kinase CK2: Interim Report from the Phase I Clinical Trial. *Eur. J. Cancer Suppl.* **2010**, *8* (7), 131–132.
- (34) Marschke, R. F.; Borad, M. J.; McFarland, R. W.; Alvarez, R. H.; Lim, J. K.; Padgett, C. S.; Von Hoff, D. D.; O'Brien, S. E.; Northfelt, D. W. Findings from the Phase I Clinical Trials of CX-4945, an Orally Available Inhibitor of CK2. *J. Clin. Oncol.* **2011**, *29*, 3087.
- (35) Zhong, B.; Campagne, O.; Salloum, R.; Purzner, T.; Stewart, C. F. LC-MS/MS Method for Quantitation of the CK2 Inhibitor Siltitasertib (CX-4945) in Human Plasma, CSF, and Brain Tissue, and Application to a Clinical Pharmacokinetic Study in Children with Brain Tumors. *J. Chromatogr. B Anal. Technol. Biomed. Life Sci.* **2020**, *1152*, 122254.
- (36) Bouhaddou, M.; Memon, D.; Meyer, B.; White, K. M.; Rezelj, V. V.; Correa Marrero, M.; Polacco, B. J.; Melnyk, J. E.; Ulferts, S.; Kaake, R. M.; et al. The Global Phosphorylation Landscape of SARS-CoV-2 Infection. *Cell* **2020**, *182* (3), 685–712.
- (37) Kim, H.; Choi, K.; Kang, H.; Lee, S. Y.; Chi, S. W.; Lee, M. S.; Song, J.; Im, D.; Choi, Y.; Cho, S. Identification of a Novel Function of CX-4945 as a Splicing Regulator. *PLoS One* **2014**, *9* (4), No. e94978.
- (38) Kim, H.; Lee, K. S.; Kim, A. K.; Choi, M.; Choi, K.; Kang, M.; Chi, S. W.; Lee, M. S.; Lee, J. S.; Lee, S. Y.; et al. A Chemical with Proven Clinical Safety Rescues Down-Syndromerelated Phenotypes in through DYRK1A Inhibition. *DMM Dis. Model. Mech.* **2016**, *9* (8), 839–848.
- (39) Perea, S. E.; Reyes, O.; Puchades, Y.; Mendoza, O.; Vispo, N. S.; Torrens, I.; Santos, A.; Silva, R.; Acevedo, B.; López, E.; et al. Antitumor Effect of a Novel Proapoptotic Peptide That Impairs the Phosphorylation by the Protein Kinase 2 (Casein Kinase 2). *Cancer Res.* **2004**, *64* (19), 7127–7129.
- (40) Perea, S. E.; Baladrón, I.; Valenzuela, C.; Perera, Y. CIGB-300: A Peptide-Based Drug That Impairs the Protein Kinase CK2-Mediated Phosphorylation. *Semin. Oncol.* **2018**, *45* (1–2), 58–67.
- (41) Perera, Y.; Ramos, Y.; Padrón, G.; Caballero, E.; Guirola, O.; Caligiuri, L. G.; Lorenzo, N.; Gottardo, F.; Farina, H. G.; Filhol, O.; et al. CIGB-300 Anticancer Peptide Regulates the Protein Kinase CK2-Dependent Phosphoproteome. *Mol. Cell. Biochem.* **2020**, *470* (1–2), 63–75.
- (42) Cruz, L. R.; Baladrón, I.; Rittoles, A.; Díaz, P. A.; Valenzuela, C.; Santana, R.; Vázquez, M. M.; García, A.; Chacón, D.; Thompson, D.; et al. Treatment with an Anti-CK2 Synthetic Peptide Improves Clinical Response in COVID-19 Patients with Pneumonia. A Randomized and Controlled Clinical Trial. *ACS Pharmacol. Transl. Sci.* **2021**, *4* (1), 206–212.
- (43) Battistutta, R.; De Moliner, E.; Sarno, S.; Zanotti, G.; Pinna, L. A. Structural Features Underlying Selective Inhibition of Protein Kinase CK2 by ATP Site-Directed Tetrabromo-2-Benzotriazole. *Protein Sci.* **2001**, *10* (11), 2200–2206.
- (44) Zandomeni, R. O. Kinetics of Inhibition of 5,6-Dichloro-1- β -D-Ribofuranosylbenzimidazole on Calf Thymus Casein Kinase II. *Biochem. J.* **1989**, *262* (2), 469–473.
- (45) Andrzejewska, M.; Pagano, M. A.; Meggio, F.; Brunati, A. M.; Kazimierzczuk, Z. Polyhalogenbenzimidazoles: Synthesis and Their Inhibitory Activity against Casein Kinases. *Bioorg. Med. Chem.* **2003**, *11* (18), 3997–4002.
- (46) Pagano, M. A.; Andrzejewska, M.; Ruzzene, M.; Sarno, S.; Cesaro, L.; Bain, J.; Elliott, M.; Meggio, F.; Kazimierzczuk, Z.; Pinna, L. A. Optimization of Protein Kinase CK2 Inhibitors Derived from 4,5,6,7-Tetrabromobenzimidazole. *J. Med. Chem.* **2004**, *47* (25), 6239–6247.
- (47) McCarty, M. F.; Assanga, S. I.; Lujan, L. L. Flavones and Flavonols May Have Clinical Potential as CK2 Inhibitors in Cancer Therapy. *Med. Hypotheses* **2020**, *141* (April), 109723.
- (48) Cozza, G.; Venerando, A.; Sarno, S.; Pinna, L. A. The Selectivity of CK2 Inhibitor Quinalizarin: A Reevaluation. *Biomed Res. Int.* **2015**, *2015*, 734127.
- (49) Cozza, G.; Zonta, F.; Dalle Vedove, A.; Venerando, A.; Dall'Acqua, S.; Battistutta, R.; Ruzzene, M.; Lolli, G. Biochemical and

Cellular Mechanism of Protein Kinase CK2 Inhibition by Deceptive Curcumin. *FEBS J.* **2020**, *287* (9), 1850–1864.

(50) Dalle Vedove, A.; Zonta, F.; Zanforlin, E.; Demitri, N.; Ribaud, G.; Cazzanelli, G.; Ongaro, A.; Sarno, S.; Zagotto, G.; Battistutta, R.; et al. A Novel Class of Selective CK2 Inhibitors Targeting Its Open Hinge Conformation. *Eur. J. Med. Chem.* **2020**, *195*, 112267.

(51) Ferguson, A. D.; Sheth, P. R.; Basso, A. D.; Paliwal, S.; Gray, K.; Fischmann, T. O.; Le, H. V. Structural Basis of CX-4945 Binding to Human Protein Kinase CK2. *FEBS Lett.* **2011**, *585* (1), 104–110.

(52) Davis-Gilbert, Z. W.; Krämer, A.; Dunford, J. E.; Howell, S.; Senbabaoglu, F.; Wells, C. I.; Bashore, F. M.; Havener, T. M.; Smith, J. L.; Hossain, M. A.; et al. Discovery of a Potent and Selective Naphthyridine-Based Chemical Probe for Casein Kinase 2. *ACS Med. Chem. Lett.* **2023**, *14* (4), 432–441.

(53) Wells, C. I.; Drewry, D. H.; Pickett, J. E.; Tjaden, A.; Krämer, A.; Müller, S.; Gyenis, L.; Menyhart, D.; Litchfield, D. W.; Knapp, S.; et al. Development of a Potent and Selective Chemical Probe for the Pleiotropic Kinase CK2. *Cell Chem. Biol.* **2021**, *28* (4), 546–558.

(54) Wells, C.; Drewry, D. H.; Pickett, J. E.; Axtman, A. D. SGC-CK2-1: The First Selective Chemical Probe for the Pleiotropic Kinase CK2. *ChemRxiv*, May 18, 2020, ver. 2. DOI: 10.26434/chemrxiv.12296180.v2.

(55) Yang, X.; Ong, H. W.; Dickmander, R. J.; Smith, J. L.; Brown, J. W.; Tao, W.; Chang, E.; Moorman, N. J.; Axtman, A. D.; Willson, T. M. Optimization of 3-Cyano-7-Cyclopropylamino-Pyrazolo [1, 5-a] Pyrimidines Toward the Development of an In Vivo Chemical Probe for CSNK2A. *ACS Omega* **2023**, *8*, 39546–39561.

(56) Krämer, A.; Kurz, C. G.; Berger, B. T.; Celik, I. E.; Tjaden, A.; Greco, F. A.; Knapp, S.; Hanke, T. Optimization of Pyrazolo[1,5-a]Pyrimidines Lead to the Identification of a Highly Selective Casein Kinase 2 Inhibitor. *Eur. J. Med. Chem.* **2020**, *208*, 112770.

(57) Uraikov, G. V.; Savateev, K. V.; Kotovskaya, S. K.; Rusinov, V. L.; Spasov, A. A.; Babkov, D. A.; Sokolova, E. V. 6-(Tetrazol-5-Yl)-7-Aminoazolo[1,5-a]Pyrimidines as Novel Potent CK2 Inhibitors. *Molecules* **2022**, *27*, 8697.

(58) Chojnacki, K.; Lindenblatt, D.; Wińska, P.; Wielechowska, M.; Toelzer, C.; Niefind, K.; Bretner, M. Synthesis, Biological Properties and Structural Study of New Halogenated Azolo[4,5-b]Pyridines as Inhibitors of CK2 Kinase. *Bioorg. Chem.* **2021**, *106*, 104502.

(59) Wasik, R.; Wińska, P.; Poznański, J.; Shugar, D. Isomeric Mono-, Di-, and Tri-Bromobenzo-1H-Triazoles as Inhibitors of Human Protein Kinase CK2 α . *PLoS One* **2012**, *7* (11), No. e48898.

(60) Winiewska, M.; Makowska, M.; Maj, P.; Wielechowska, M.; Bretner, M.; Poznański, J.; Shugar, D. Thermodynamic Parameters for Binding of Some Halogenated Inhibitors of Human Protein Kinase CK2. *Biochem. Biophys. Res. Commun.* **2015**, *456* (1), 282–287.

(61) Winiewska-Szajewska, M.; Maciejewska, A. M.; Speina, E.; Poznański, J.; Paprocki, D. Synthesis of Novel Halogenated Heterocycles Based on O-phenylenediamine and Their Interactions with the Catalytic Subunit of Protein Kinase Ck2. *Molecules* **2021**, *26* (11), 3163.

(62) Morooka, S.; Hoshina, M.; Kii, I.; Okabe, T.; Kojima, H.; Inoue, N.; Okuno, Y.; Denawa, M.; Yoshida, S.; Fukuhara, J.; et al. Identification of a Dual Inhibitor of SRPK1 and CK2 That Attenuates Pathological Angiogenesis of Macular Degeneration in Mice. *Mol. Pharmacol.* **2015**, *88* (2), 316–325.

(63) Nishiwaki, K.; Nakamura, S.; Yoshioka, K.; Nakagawa, E.; Nakatani, S.; Tsuyuguchi, M.; Kinoshita, T.; Nakanishi, I. Design, Synthesis and Structure-Activity Relationship Studies of Protein Kinase CK2 Inhibitors Containing a Purine Scaffold. *Chem. Pharm. Bull. (Tokyo)* **2023**, *71* (7), 558–565.

(64) López-Rojas, P.; Haidar, S.; Jürgens, F. M.; Aichele, D.; Amesty, A.; Estévez-Braun, A.; Jose, J. Synthesis and Biological Evaluation of Anthracene-9,10 Dione Derivatives as CK2 Inhibitors. *Results Chem.* **2023**, *6* (June), 100997.

(65) Bestgen, B.; Krimm, I.; Kufareva, I.; Kamal, A. A. M.; Seetoh, W. G.; Abell, C.; Hartmann, R. W.; Abagyan, R.; Cochet, C.; Le Borgne, M.; et al. 2-Aminothiazole Derivatives as Selective Allosteric

Modulators of the Protein Kinase CK2. 1. Identification of an Allosteric Binding Site. *J. Med. Chem.* **2019**, *62* (4), 1803–1816.

(66) Bestgen, B.; Kufareva, I.; Seetoh, W.; Abell, C.; Hartmann, R. W.; Abagyan, R.; Le Borgne, M.; Filhol, O.; Cochet, C.; Lomberget, T.; et al. 2-Aminothiazole Derivatives as Selective Allosteric Modulators of the Protein Kinase CK2. 2. Structure-Based Optimization and Investigation of Effects Specific to the Allosteric Mode of Action. *J. Med. Chem.* **2019**, *62* (4), 1817–1836.

(67) Lindenblatt, D.; Nickelsen, A.; Applegate, V. M.; Jose, J.; Niefind, K. Structural and Mechanistic Basis of the Inhibitory Potency of Selected 2-Aminothiazole Compounds on Protein Kinase CK2. *J. Med. Chem.* **2020**, *63* (14), 7766–7772.

(68) Brear, P.; Ball, D.; Stott, K.; D'Arcy, S.; Hyvonen, M. Proposed Allosteric Inhibitors Bind to the ATP Site of CK2 α . *J. Med. Chem.* **2020**, *63*, 12786–12798.

(69) Oshima, T.; Niwa, Y.; Kuwata, K.; Srivastava, A.; Hyoda, T.; Tsuchiya, Y.; Kumagai, M.; Tsuyuguchi, M.; Tamaru, T.; Sugiyama, A.; et al. Cell-Based Screen Identifies a New Potent and Highly Selective CK2 Inhibitor for Modulation of Circadian Rhythms and Cancer Cell Growth. *Sci. Adv.* **2019**, *5* (1), No. eaau9060.

(70) Chen, X.; Li, C.; Wang, D.; Chen, Y.; Zhang, N. Recent Advances in the Discovery of CK2 Allosteric Inhibitors: From Traditional Screening to Structure-Based Design. *Molecules* **2020**, *25* (4), 870.

(71) Jiang, H.; Dong, J.; Song, K.; Wang, T.; Huang, W.; Zhang, J.; et al. A Novel Allosteric Site in Casein Kinase 2 α Discovered Using Combining Bioinformatics and Biochemistry Methods. *Acta Pharmacol. Sin.* **2017**, *38*, 1691–1698.

(72) Raaf, J.; Brunstein, E.; Issinger, O. G.; Niefind, K. The CK2 α /CK2 β Interface of Human Protein Kinase CK2 Harbors a Binding Pocket for Small Molecules. *Chem. Biol.* **2008**, *15* (2), 111–117.

(73) Prudent, R.; Cochet, C. New Protein Kinase CK2 Inhibitors: Jumping out of the Catalytic Box. *Chem. Biol.* **2009**, *16* (2), 112–120.

(74) Laudet, B.; Barette, C.; Dulery, V.; Renaudet, O.; Dumy, P.; Metz, A.; Prudent, R.; Deshiere, A.; Dideberg, O.; Filhol, O.; et al. Structure-Based Design of Small Peptide Inhibitors of Protein Kinase CK2 Subunit Interaction. *Biochem. J.* **2007**, *408* (3), 363–373.

(75) Lindenblatt, D.; Horn, M.; Götz, C.; Niefind, K.; Neundorff, I.; Pietsch, M. Design of CK2 β -Mimicking Peptides as Tools To Study the CK2 α /CK2 β Interaction in Cancer Cells. *ChemMedChem.* **2019**, *14*, 833–841.

(76) Iegre, J.; Brear, P.; Baker, D. J.; Tan, Y. S.; Atkinson, E. L.; Sore, H. F.; O'Donovan, D. H.; Verma, C. S.; Hyvönen, M.; Spring, D. R. Efficient Development of Stable and Highly Functionalised Peptides Targeting the CK2 α /CK2 β Protein-Protein Interaction. *Chem. Sci.* **2019**, *10* (19), 5056–5063.

(77) Bestgen, B.; Belaid-Choucair, Z.; Lomberget, T.; Le Borgne, M.; Filhol, O.; Cochet, C. In Search of Small Molecule Inhibitors Targeting the Flexible CK2 Subunit Interface. *Pharmaceuticals* **2017**, *10* (1), 16.

(78) Brear, P.; North, A.; Iegre, J.; Hadje Georgiou, K.; Lubin, A.; Carro, L.; Green, W.; Sore, H. F.; Hyvönen, M.; Spring, D. R. Novel Non-ATP Competitive Small Molecules Targeting the CK2 α / β Interface. *Bioorg. Med. Chem.* **2018**, *26* (11), 3016–3020.

(79) Brear, P.; De Fusco, C.; Hadje Georgiou, K.; Francis-Newton, N. J.; Stubbs, C. J.; Sore, H. F.; Venkitaraman, A. R.; Abell, C.; Spring, D. R.; Hyvönen, M. Specific Inhibition of CK2 α from an Anchor Outside the Active Site. *Chem. Sci.* **2016**, *7* (11), 6839–6845.

(80) De Fusco, C.; Brear, P.; Iegre, J.; Georgiou, K. H.; Sore, H. F.; Hyvönen, M.; Spring, D. R. A Fragment-Based Approach Leading to the Discovery of a Novel Binding Site and the Selective CK2 Inhibitor CAM4066. *Bioorg. Med. Chem.* **2017**, *25* (13), 3471–3482.

(81) Iegre, J.; Brear, P.; De Fusco, C.; Yoshida, M.; Mitchell, S. L.; Rossmann, M.; Carro, L.; Sore, H. F.; Hyvönen, M.; Spring, D. R. Second-Generation CK2 α Inhibitors Targeting the Ad Pocket. *Chem. Sci.* **2018**, *9* (11), 3041–3049.

(82) Viht, K.; Saaver, S.; Vahter, J.; Enkvist, E.; Lavogina, D.; Sinijärvi, H.; Raidaru, G.; Guerra, B.; Issinger, O. G.; Uri, A. Acetoxymethyl Ester of Tetrabromobenzimidazole-Peptoid Conjugate

for Inhibition of Protein Kinase CK2 in Living Cells. *Bioconjugate Chem.* **2015**, *26* (12), 2324–2335.

(83) Li, C.; Zhang, X.; Zhang, N.; Zhou, Y.; Sun, G.; Zhao, L.; Zhong, R. Identification and Biological Evaluation of CK2 Allosteric Fragments through Structure-Based Virtual Screening. *Molecules* **2020**, *25* (1), 237.

(84) Lindenblatt, D.; Applegate, V.; Nickelsen, A.; Klußmann, M.; Neundorff, I.; Götz, C.; Jose, J.; Niefind, K. Molecular Plasticity of Crystalline CK2 α' Leads to KN2, a Bivalent Inhibitor of Protein Kinase CK2 with Extraordinary Selectivity. *J. Med. Chem.* **2022**, *65* (2), 1302–1312.

(85) Pietsch, M.; Viht, K.; Schnitzler, A.; Ekambaram, R.; Steinkrüger, M.; Enkvist, E.; Nienberg, C.; Nickelsen, A.; Lauwers, M.; Jose, J.; et al. Unexpected CK2 β -Antagonistic Functionality of Bisubstrate Inhibitors Targeting Protein Kinase CK2. *Bioorg. Chem.* **2020**, *96*, 103608.

(86) Kufareva, I.; Bestgen, B.; Brear, P.; Prudent, R.; Laudet, B.; Moucadel, V.; Ettaoussi, M.; Sautel, C. F.; Krimm, I.; Engel, M.; et al. Discovery of Holoenzyme-Disrupting Chemicals as Substrate-Selective CK2 Inhibitors. *Sci. Rep.* **2019**, *9* (1), 15893.

(87) Martinez, R.; Di Geronimo, B.; Pastor, M.; Zapico, J. M.; Coderch, C.; Panchuk, R.; Skorokhyd, N.; Maslyk, M.; Ramos, A.; De Pascual-teresa, B. Multitarget Anticancer Agents Based on Histone Deacetylase and Protein Kinase CK2 Inhibitors. *Molecules* **2020**, *25*, 1497.

(88) Rangasamy, L.; Ortín, I.; Zapico, J. M.; Coderch, C.; Ramos, A.; De Pascual-Teresa, B. New Dual CK2/HDAC1 Inhibitors with Nanomolar Inhibitory Activity against Both Enzymes. *ACS Med. Chem. Lett.* **2020**, *11* (5), 713–719.

(89) Chen, F.; Pei, S.; Wang, X.; Zhu, Q.; Gou, S. Emerging JWA-Targeted Pt(IV) Prodrugs Conjugated with CX-4945 to Overcome Chemo-Immune-Resistance. *Biochem. Biophys. Res. Commun.* **2020**, *521* (3), 753–761.

(90) Wang, Y.; Wang, X.; Xu, G.; Gou, S. Novel CK2-Specific Pt(II) Compound Reverses Cisplatin-Induced Resistance by Inhibiting Cancer Cell Stemness and Suppressing DNA Damage Repair in Non-Small Cell Lung Cancer Treatments. *J. Med. Chem.* **2021**, *64* (7), 4163–4178.

(91) Wang, Y.; Lv, Z.; Chen, F.; Wang, X.; Gou, S. Discovery of 5-(3-Chlorophenylamino)Benzo[*c*][2,6]Naphthyridine Derivatives as Highly Selective CK2 Inhibitors with Potent Cancer Cell Stemness Inhibition. *J. Med. Chem.* **2021**, *64* (8), 5082–5098.

(92) Zhang, J.; Tang, P.; Zou, L.; Zhang, J.; Chen, J.; Yang, C.; He, G.; Liu, B.; Liu, J.; Chiang, C. M.; et al. Discovery of Novel Dual-Target Inhibitor of Bromodomain-Containing Protein 4/Casein Kinase 2 Inducing Apoptosis and Autophagy-Associated Cell Death for Triple-Negative Breast Cancer Therapy. *J. Med. Chem.* **2021**, *64* (24), 18025–18053.

(93) Chojnacki, K.; Wińska, P.; Wielechowska, M.; Łukowska-Chojnacka, E.; Tölzer, C.; Niefind, K.; Bretner, M. Biological Properties and Structural Study of New Aminoalkyl Derivatives of Benzimidazole and Benzotriazole, Dual Inhibitors of CK2 and PIM1 Kinases. *Bioorg. Chem.* **2018**, *80*, 266–275.

(94) Wińska, P.; Wielechowska, M.; Koronkiewicz, M.; Borowiecki, P. Synthesis and Anticancer Activity of Novel Dual Inhibitors of Human Protein Kinases CK2 and PIM-1 †. *Pharmaceutics* **2023**, *15* (7), 1991.

(95) Al-Qadhi, M. A.; Allam, H. A.; Fahim, S. H.; Yahya, T. A. A.; Ragab, F. A. F. Design and Synthesis of Certain 7-Aryl-2-Methyl-3-Substituted Pyrazolo{1,5-A}Pyrimidines as Multikinase Inhibitors. *Eur. J. Med. Chem.* **2023**, *262*, 115918.

(96) Al-Dhuayan, I.; ALaqeel, N. K. Molecular Docking, ADMET and Molecular Dynamics Simulation Revealed Metralindole as a Multitargeted Inhibitor for Division Kinases. *Braz. J. Biol.* **2023**, *83*, No. e271688.

(97) Goudzal, A.; El Aissouq, A.; El Hamdani, H.; Hadaji, E. G.; Ouammou, B.; Bouachrine, M. 3D-QSAR Modeling and Molecular Docking Studies on a Series of 2, 4, 5-Trisubstituted Imidazole

Derivatives as CK2 Inhibitors. *J. Biomol. Struct. Dyn.* **2023**, *41*, 234–248.

(98) Yadav, S.; Ahamad, S.; Gupta, D.; Mathur, P. Lead Optimization, Pharmacophore Development and Scaffold Design of Protein Kinase CK2 Inhibitors as Potential COVID-19 Therapeutics. *J. Biomol. Struct. Dyn.* **2023**, *41* (5), 1811–1827.

(99) Patel, S.; Patel, S.; Tulsian, K.; Kumar, P.; Vyas, V. K.; Ghate, M. Design of 2-Amino-6-Methyl-Pyrimidine Benzoic Acids as ATP Competitive Casein Kinase-2 (CK2) Inhibitors Using Structure- and Fragment-Based Design, Docking and Molecular Dynamic Simulation Studies. *SAR QSAR Environ. Res.* **2023**, *34* (3), 211–230.